Review

Technology and Applications of Wide Bandgap Semiconductor Materials: Current State and Future Trends

Omar Sarwar Chaudhary [1], Mouloud Denaï [1,*], Shady S. Refaat [1,2] and Georgios Pissanidis [3]

1 School of Physics, Engineering and Computer Science, University of Hertfordshire, Hatfield AL10 9AB, UK; o.s.chaudhary2@herts.ac.uk (O.S.C.); s.khalil3@herts.ac.uk (S.S.R.)
2 Department of Electrical and Computer Engineering, Texas A&M University at Qatar, Doha 23874, Qatar
3 Enoda Ltd., Edinburgh EH3 9EG, UK; g.pissanidis@enodatech.com
* Correspondence: m.denai@herts.ac.uk

Abstract: Silicon (Si)-based semiconductor devices have long dominated the power electronics industry and are used in almost every application involving power conversion. Examples of these include metal-oxide-semiconductor field-effect transistors (MOSFETs), insulated-gate bipolar transistors (IGBTs), gate turn-off (GTO), thyristors, and bipolar junction transistor (BJTs). However, for many applications, power device requirements such as higher blocking voltage capability, higher switching frequencies, lower switching losses, higher temperature withstand, higher power density in power converters, and enhanced efficiency and reliability have reached a stage where the present Si-based power devices cannot cope with the growing demand and would usually require large, costly cooling systems and output filters to meet the requirements of the application. Wide bandgap (WBG) power semiconductor materials such as silicon carbide (SiC), gallium nitride (GaN), and diamond (Dia) have recently emerged in the commercial market, with superior material properties that promise substantial performance improvements and are expected to gradually replace the traditional Si-based devices in various power electronics applications. WBG power devices can significantly improve the efficiency of power electronic converters by reducing losses and making power conversion devices smaller in size and weight. The aim of this paper is to highlight the technical and market potential of WBG semiconductors. A detailed short-term and long-term analysis is presented in terms of cost, energy impact, size, and efficiency improvement in various applications, including motor drives, automotive, data centers, aerospace, power systems, distributed energy systems, and consumer electronics. In addition, the paper highlights the benefits of WBG semiconductors in power conversion applications by considering the current and future market trends.

Keywords: Wide Bandgap Semiconductor; semiconductor materials; power electronic devices

Citation: Chaudhary, O.S.; Denaï, M.; Refaat, S.S.; Pissanidis, G. Technology and Applications of Wide Bandgap Semiconductor Materials: Current State and Future Trends. *Energies* **2023**, *16*, 6689. https://doi.org/10.3390/en16186689

Academic Editors: Massimiliano Luna and Marcello Pucci

Received: 27 July 2023
Revised: 11 September 2023
Accepted: 13 September 2023
Published: 18 September 2023

Copyright: © 2023 by the authors. Licensee MDPI, Basel, Switzerland. This article is an open access article distributed under the terms and conditions of the Creative Commons Attribution (CC BY) license (https://creativecommons.org/licenses/by/4.0/).

1. Introduction

Power electronics has been the key technology driver for efficient electrical power conversion for more than two decades, covering a breadth of application areas ranging from aerospace, automotive, consumer electronics, industry, utility systems, and many other areas. It is estimated that by 2030, around 80% of the worldwide energy generation and consumption will be processed through power electronics [1]. While, in the case of many renewable energy applications, including solar photovoltaic (PV) inverters, 100% of the electrical energy is processed by a power converter consisting of different switching devices. As global demand for energy continues to rise due to economic growth and population increase, improvement in energy efficiency has become a crucial challenge. The largest amount of power losses that occurs in power electronic converters is dissipated in the power semiconductor devices. Currently, even with these various limitations, the mature and very well-established Si-based technology is still playing a leading role in satisfying the constantly growing demands of power semiconductor devices [2]. A bibliometric

analysis based on a thesaurus file from the dimension's website was conducted to shape the review structure, as illustrated in Figure 1. The proposed bibliometric visualization for the author-supplied keywords was created with VOS viewer software from 2018 to 2023. It shows three topic clusters: WBG semiconductor materials, technology and applications, and current state and future trends.

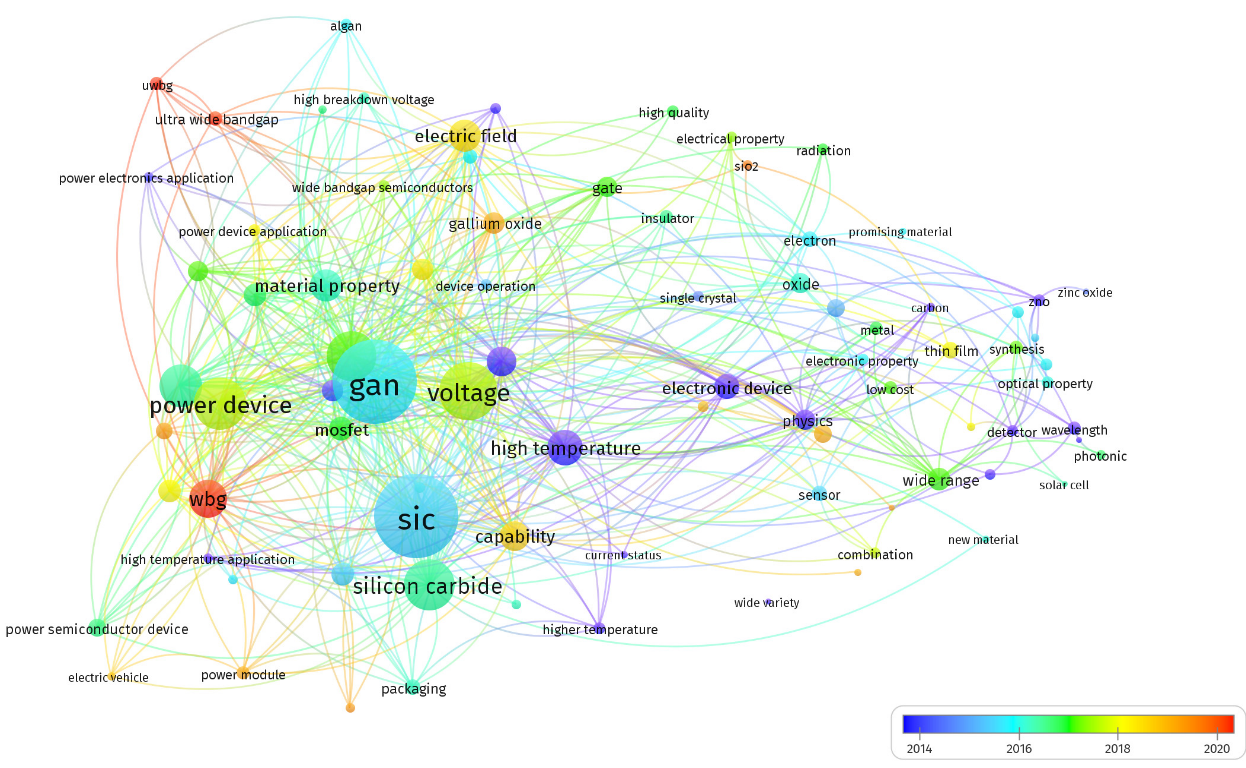

Figure 1. Bibliometric analysis of author-supplied keywords, with node size indicating frequency of recurrence and node connections indicating co-occurrence within the same quartile.

Si-based devices are widely used in power converters, which include bipolar, unipolar, controlled, and uncontrolled devices. Examples of such devices are power diodes, thyristors (gate turn-offs (GTO); gate-controlled thyristors (GCT)), BJTs (bipolar junction transistors), IGBTs, and MOSFETs. A new generation of IGBTs is now able to handle voltages up to 6.5 kV and currents up to 1700 A. The IGBT (insulated gate bipolar transistor) represents a power semiconductor device comprising four layers and three terminals. It serves as a merged unit combining the attributes of power MOSFET and BJT, facilitating rapid switching and elevated power-handling capacity. The IGBT is characterized by its capability to deliver efficient switching with minimal power loss in the ON state, along with superior ratings when compared to both MOSFET and BJT devices. IGBTs are commonly used in motor drives, converters circuits, and power supplies applications where there is a demand for high voltage and currents. Power MOSFETs, on the other hand, are increasingly used by the power supply community and in low-power inverters due to their high switching ability and ease of drive circuitry in contrast to IGBTs [3]. Si-based MOSFETs have long been hindered due to their high on-state resistance, which substantially increases power losses in the devices. The on-state resistance increases in proportion with the blocking voltage, which makes them unsuitable for high-voltages applications above 600 V [4].

The physical limitations of the current generation of Si-based MOSFETs and IGBTs have hindered the progress in achieving high efficiency, reliability, and compact form factor in power applications. It is desirable to convert power at high frequencies for power converters and other electronic system applications. There are many advantages when switching at higher frequencies, such as a reduction in the size, weight, and cost of the converter. The limitation of Si-based power semiconductors arises due to a decrease in

efficiency and a substantial increase in temperature stress cycles as the switching frequency increases [5].

Technical Challenges Facing Si Semiconductor Devices

The design and fabrication of Si power devices with enhanced functionality, efficiency, and reliability offer several benefits and advantages in numerous areas, especially for efficient grid integration of renewable and distributed energy sources. Additionally, the integration of Si power devices in advanced converters topologies offers tremendous benefits in terms of cost of energy, improvement in efficiency, and converter size reduction. To achieve higher efficiencies in power conversion applications, semiconductor switches must exhibit the lowest power losses. Currently, Si-based switches such as MOSFETs, IGBTs, and thyristors have many limitations in terms of design and material properties, which tend to affect the overall performance of the power conversion application [6].

High Losses: Since Si has a low bandgap (1.1 eV) and low critical electric field (30 MV/cm), the thickness of the device will increase considerably with high voltages, which leads to high resistance and consequently increased conduction losses. Also, in critical applications, the low bandgap of Si affects its robustness against disturbances such as intense magnetic fields, radiation, and heat.

Low Switching Frequency: Si-based power MOSFETs exhibit relatively high losses at higher switching frequencies due to increased die size. This large die surface area is designed to minimize conductions, but it results in higher gate capacitance and the generation of large peak currents from gate charge, which in turn increases the switching losses at higher frequencies. Si-based IGBTs have a smaller die surface area than MOSFETs, as they utilize minority carriers for conductivity modulation. However, the long lifetime of minority carriers decreases the overall frequency range. Thus, at higher frequencies, both MOSFETs and IGBTs exhibit higher losses and are often operated at lower switching frequencies, which is not advantageous in many power applications; hence, this impacts the overall efficiency of power applications and devices.

Poor Performance at High Temperature: The low Si bandgap also contributes to high intrinsic carrier concentrations in Si-based devices. This translates into increased leakage currents at higher temperatures. Temperature variation of the bipolar gain in IGBTs amplifies the leakage and limits the maximum junction temperature of many IGBTs to 125 °C [7]. Due to this fact, current systems with Si-based semiconductors require expensive and bulky cooling systems for heat removal. There are many areas where power semiconductors are operated at high temperatures, such as military, aerospace, high-power applications, and optoelectronics. The High-Temperature Electronics Network of Excellence (HITEN) has estimated the high-temperature electronics market's worth around USD 9.5 billion, and it is expected to grow above USD 19.5 billion [8]. Recently, there has been extensive and ongoing research and development on the design of advanced and effective cooling systems for power electronics components. Smart cooling systems can considerably increase the lifetime and efficiency of semiconductor devices by operating the device within its physical limits. In many high-power electronics applications, micro-cooling systems comprising chip control, integrated control loops, liquid cooling systems, and temperature sensors are designed to effectively remove the excessive heat from the device. The reliability, efficiency, and lifetime of semiconductor materials decrease when operated under high temperatures and various stress conditions. Table 1 shows the effects of temperature on selected major sensors and semiconductor devices [9].

Table 1. Effect of temperature on major semiconductor devices [9].

Major Semiconductor Devices	Effect of High Temperature (T)
Thermistor	▪ Number of charge carriers and conductivity increases
Piezo-resistive sensors with PN insulation	▪ Sensitivity decreases ▪ Junction leakage current increases

Table 1. *Cont.*

Major Semiconductor Devices	Effect of High Temperature (T)
Schottky diodes	▪ Forward voltage-drop decreases ▪ Reverse current increases with T^2
PN diodes	▪ Voltage drop in the forward direction decreases ▪ Leakage current increases exponentially
Bipolar transistor	▪ Base-emitter voltage decreases at collector current ▪ Current amplification increases with T^x $(1 < x < 2)$
JFET	▪ Channel mobility decreases with $T^{3/2}$ ▪ Pinch-off voltage increases
MESFET	▪ Similar to JFET
MOSFET	▪ Channel mobility decreases with $T^{3/2}$ ▪ Leakage current of PN junctions increases exponentially ▪ Threshold voltage decreases

2. WBG Material Properties and Market Trend

In the last decade, numerous improvements have been made to the existing silicon technology in terms of structure, design, and material properties. As the demand for higher current, voltage, packaging density, and temperature is constantly growing, Si-based power devices have gradually started approaching their performance limits. While, WBG semiconductors have begun to emerge as a potential alternative technology. They offer better inherent material advantages over Si, such as higher voltage breakdown, higher switching frequency, comparable carrier mobility, higher energy bandgap, and higher thermal conductivity [10].

WBG-based semiconductors such as silicon carbide (SiC), gallium nitride (GaN), and diamond (Dia) are superior to Si semiconductors and offer many advantages for power conversion applications. The physical characteristics of SiC, GaN, and Dia, include higher bandgap width (3~4 times), higher breakdown field (4–20 times), higher thermal conductivity (3–13 times), larger saturated electron drift velocity, low intrinsic carrier concentration (between 10–35 order of magnitude), and higher bandgap energy as compared to those of Si [3]. Figure 2 illustrates the thermal, voltage, and frequency characteristics of Si, SiC, and GaN materials.

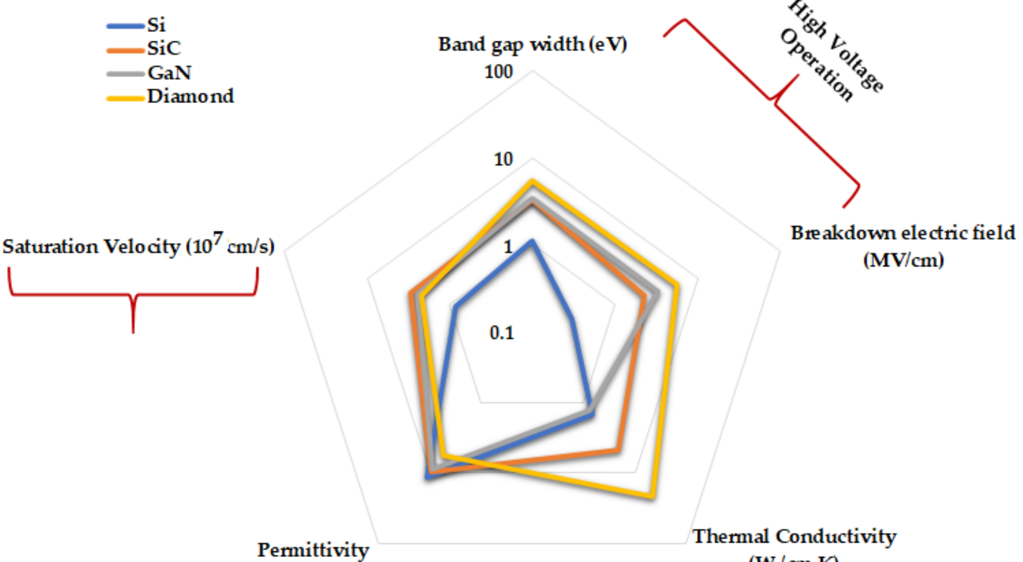

Figure 2. Si, SiC, and GaN properties.

Other advantages of WBG semiconductors are their thinner drift regions due to increased electric critical field value, which can result in lower on-resistance and better coefficient of

thermal expansion (CTE). Materials having CTE closer to the available electrically insulating and thermally conductive ceramics layers can be adopted more easily for higher power and temperature applications compared to Si. There are also some disadvantages of WBG semiconductors, such as their electrons and holes mobility, which might in some cases make them inappropriate for bipolar devices. For high-power and high-temperature applications, WBG semiconductors offer physical properties relatively superior to those of Si-based semiconductor technology. As temperature increases, the degradation of the semiconductor material will continue until it fails to provide sufficient functionality. There are certain amount of thermal electron and hole carriers called intrinsic carriers. As temperature increases, the number of carriers increases exponentially, which causes a degradation in the electrical conductivity of the doped regions in Si-based semiconductors. The other source of degradation is due to the P–N junction leakage current, which is directly related to the intrinsic concentration of the semiconductor. Since WBG semiconductors have lower intrinsic carrier concentration, the leakage currents are smaller as compared to silicon. Another fundamental mechanism in semiconductors is the ability of carriers to move through the semiconductor. When the temperature increases, the ability of carriers to move inside the crystal decreases. This is due to atoms in the crystal lattice acquiring more energy as the temperature increases, hence increasing the thermal vibrational energy that results in more collisions through the crystal. This leads to a reduction in the amount of current that a diode or a transistor can carry due to a decrease in carrier mobility [11]. With the combination of improved material properties, WBG can significantly reduce losses by 95% up to 98% or higher depending on the application [12]. This substantially reduces the cooling requirements and size of passive components, leading to a reduction in size, weight, and cost [13].

Despite all these advantages, SiC-, GaN-, and Dia-based semiconductors are still in their early stages of research and development. Because of its higher thermal conductivity, ultrawide bandgap, and higher carrier mobility as compared to other semiconductors, Dia is set to become the best semiconductor material in the future. Even though Dia is the best semiconductor, the device material and fabrication technology is less mature and less developed as compared to SiC and GaN [14]. Currently, the WBG semiconductors market represents a small segment in the global power electronics industry, and power electronics in turn are small fraction of the global semiconductor market. The U.S. is leading the market share for WBG research and development, but the rising competition from Europe, China, and Japan is changing this landscape [15]. Figure 3 presents the WBG market share within the semiconductor industry. It shows that the semiconductor sales market share within the region rose from USD 337.30 billion in 2015 to USD 583.20 billion in 2022 [16], while Figure 4 illustrates the projected yearly growth of WBG market by application [17]. It shows that EV application has the highest growth compared with other applications.

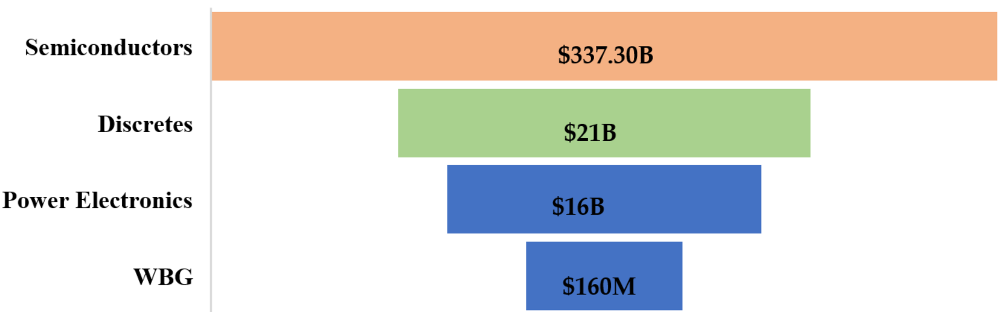

Figure 3. WBG power electronics within total semiconductor industry [16].

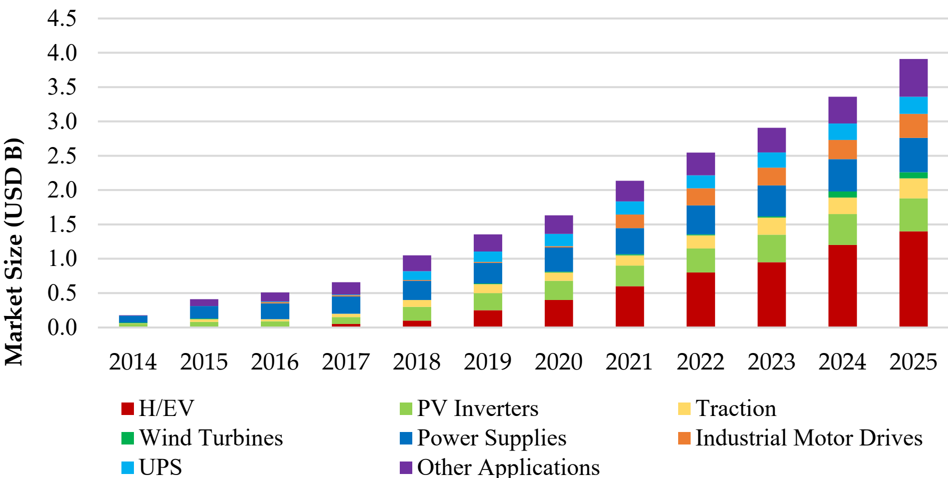

Figure 4. Projected annual growth by application of WBG market [17].

2.1. Performance Advances and Market Trends of SiC

There are many challenges that arise when developing new generation of WBG-based semiconductors for various applications. For SiC-based devices, the difficulty arises from the presence of crystal defects and lack of abundant wafers during the material processing. These factors have ultimately contributed to the slow commercial development of SiC power devices. SiC has well over 150 different polytypes, but only 6H-SiC and 4H-SiC are commercially available in the form of abundant wafers and epitaxial layers [18]. Among these two, 4H-SiC exhibits better characteristics because of its higher carrier mobility and higher electric breakdown field, which helps reduce the size of the epitaxial layers. The reduction in the size of the drift layer helps reduce the low drift resistance, which in turn reduces the forward voltage drop and conduction losses [19]. Table 2 presents a comparison between material properties of Si, 6H-SiC, and 4H-SiC semiconductors [19].

Table 2. 4H-SiC, 6H-SiC, Si, and diamond material properties [19].

Parameters	4H-SiC	6H-SiC	Si	GaN	Diamond
$E_{g(300\ K)}$ (eV)	3.26	2.90	1.12	3.39	5.47
$n_{i(300\ K)}$(cm^{-3})	1.5×10^{-8}	2.1×10^{-5}	10^{10}	2×10^{-10}	10^{-20}
$E_{crit(300\ K)}$ (V/cm)	2.2×10^{6}	2.5×10^{6}	0.25×10^{6}	3.3×10^{6}	5.6×10^{6}
ϵ_S	9.66	9.66	11.7	9.5	5.7
$\mu_{n,max}\perp$ (cm^2/Vs)	1000−1140	415	1400	1250	1800
$\mu_{p,max}\perp$ (cm^2/Vs)	124	99	450	200	
V_{SAT} (cm/s)	2.1×10^{7}	2×10^{7}	10^{7}	2.7×10^{7}	2.7×10^{7}

SiC-based semiconductors are relatively new in the power industry. The first commercial power device was introduced in 2001 as the SiC-based Schottky diode [20]. Despite being relatively new in the commercial marketplace, significant improvements have been made over the years. One of the SiC leading manufacturers, Cree, was the first to announce in 2012 the production of 150 mm SiC wafers and a range of power MOSFETs [21]. Initially, SiC wafers suffered from defects such as micropipes; however, wafer quality has improved quite significantly over these past years. The defects were in the range of 5–10/cm^2 in 2006 [22], improving to 0.75/cm^2 in 2014 [23], and recently, the Japanese manufacturer Showa Denko lowered the defect densities of 150 mm (6 inch) SiC wafers by up to 0.25/cm^2 [2]. SiC devices' cost is expected to decrease gradually as manufacturers improve the fabrication processes by improving the production capabilities and wafer sizes. Figure 5 illustrates the current and future market demand for the 150 mm SiC wafer size in comparison to 100 mm [24], while Figure 6 depicts the key milestones in the research and development in SiC technology. Due to the improvements in wafer fabrication and

increased production volumes, SiC power devices' costs have significantly declined since the introduction of first SiC Schottky diode and MOSFETs. The initial cost of the SiC Schottky diode was USD 5000 for a two-inch wafer, USD 1200–USD 1400 in 2009 for a four-inch wafer, and USD 600–USD 750 in 2012 [25]. Also, during this time span, SiC power devices sales increased by three times over the years [26].

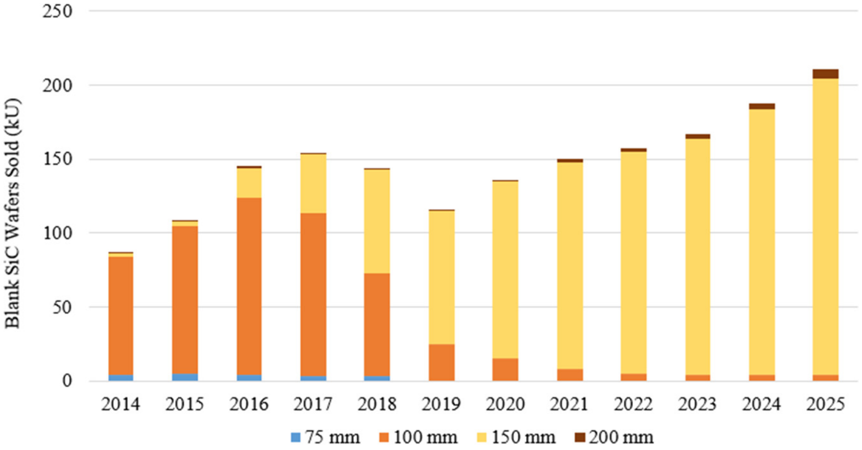

Figure 5. Production of various SiC substrate wafers.

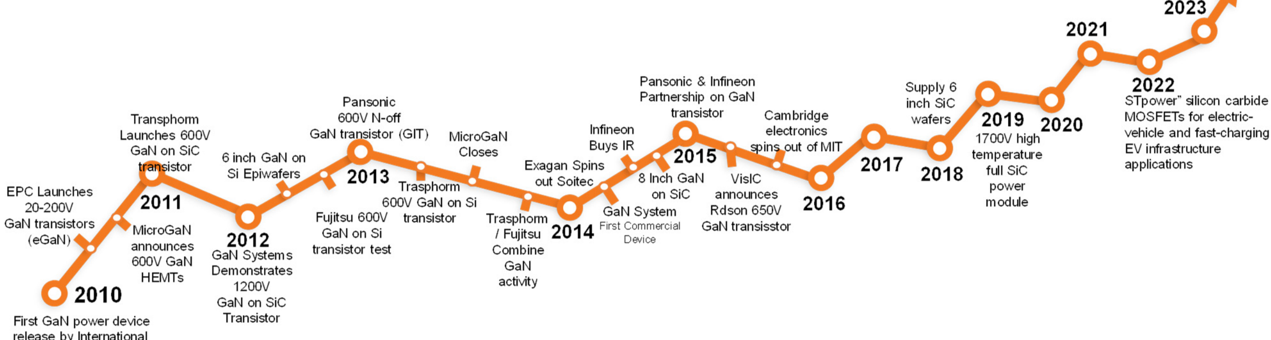

Figure 6. Milestones in SiC power electronics development.

Cree is one of the world's largest growing power semiconductor manufacturers. Figure 7 shows the Cree SiC power devices' costs trend over the past few years [27]. The performance of SiC power devices has also gradually improved over the last years since their introduction in 2001. Figure 8 illustrates the current density growth from 2010 to 2012 and a prediction of future trends up to 2020 [28]. For high-voltage SiC power devices, there is a steady increase in current density, while for lower-voltage SiC power devices, the current density is expected to slow down around the end of this decade due to the cost of SiC modules and long-term reliability [29]. In 2005, Schottky diodes were available at current rating up to 25 A; nowadays, the current ratings of these devices can reach 50 A [30]. Also, significant progress has been made in SiC power MOSFETs technology, which led to an increase in the performance of each generation of devices. Due to SiC maturity over GaN, higher breakdown voltage and current capabilities are commercially available (SiC MOSFETs available up to 1.7 kV and thyristor up to 6.5 kV), while Wolfspeed (Cree) successfully tested 10 kV MOSFETs and further developed 15 kV SiC [31]. In 2011, a 1200 V SiC MOSFET had switching losses around 0.78 mJ, and in 2013, the average switching losses of the next-generation SiC power MOSFETs were 0.56 mJ, i.e., a 28% decrease [25]. These performance enhancements were the results of the recent advances made in material development and fabrication processes [32].

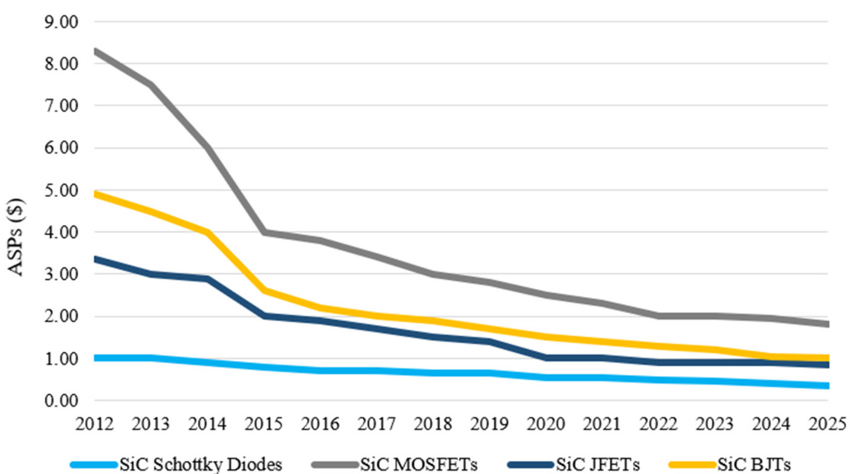

Figure 7. Decline of device cost for Cree SiC products over the last years [27].

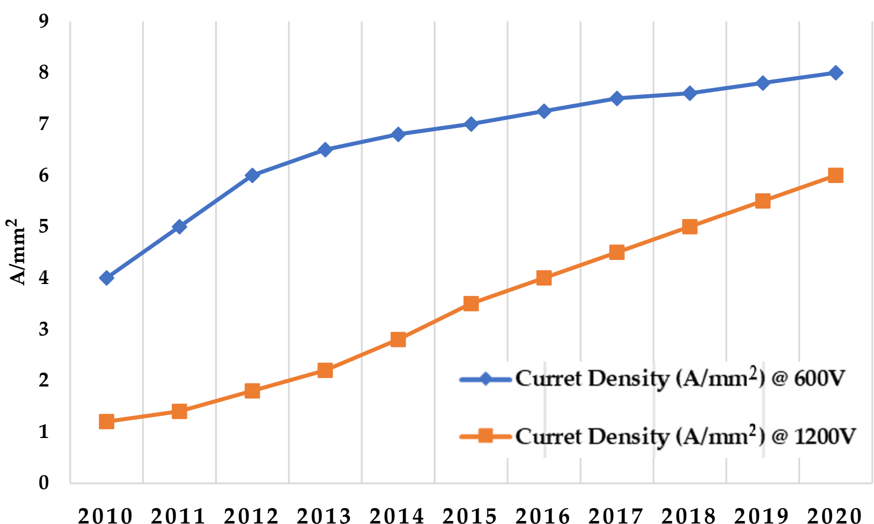

Figure 8. Current density evolution for SiC [16].

At present, SiC power electronics' technological development and production is mainly carried out by a few key companies in the market. Table 3 gives a list of these companies, their market share, and their revenue in 2010 [26]. In 2021, the global SiC power electronics industry was estimated to be worth USD 1.090 million and is due to reach USD 6.297 million by 2027 [33]. The companies leading the research and development are mainly Infineon, Mitsubishi Electric, ON Semiconductor, and STMicroelectronics. SiC fabrication facilities are mainly in Europe (55%), the United States (41%), and Japan (2%). By 2020, the market share of SiC devices is expected to shift radically, with Japan capturing 35% of the global market share due to considerable investment from the Japanese government and industry [34]. Toyota is one of the Japanese car manufacturers currently testing hybrid vehicles and buses based on SiC power devices [35].

Table 3. Distribution of leading SiC power electronics device makers by market share in 2021.

Company	SiC Power Electronics Market Growth	Headquarters
STMicroelectronics	55%	Switzerland
Infineon	126%	Germany
ON Semiconductor	43%	USA
Wolfspeed	53%	USA
Mitsubishi Electric	8%	Japan
ROHM	5%	USA

2.2. Performance Advances in GaN

GaN offers many features such as faster switching speed, smaller size, higher efficiency, and lower cost. Currently, GaN-based devices are already commercialized for lasers and RF applications, while for high-power applications, GaN technology is still at its early stage. Due to the lack of abundance of high-quality, defect-free GaN substrates, GaN epilayers are designed on foreign substrates such as Si, SiC, and sapphire. Among these, GaN epilayers grown on Si offer lower cost and better performance in comparison to the other substrate materials. AlGaN/GaN heterostructure field-effect transistors (HFETs) and high electron mobility transistor (HEMTs) have been commercially available since 2005 and have mostly been used in RF and optoelectronics. Recently, many power electronic design companies have opted for AlGaN/GaN HEMTs in various power applications, such as power converters. The most interesting property is the existence of two-dimensional electron gas (2DEG) formed in AlGaN/GaN structures due to the discontinuity difference between GaN and AlGaN. 2DEG is a gas of electrons free to move in two dimensions but tightly confined in the third. This tight confinement leads to quantized energy levels for motion in the third direction. Also, due to presence of polarization fields for AlGaN/GaN HEMTs, this allows for a high 2DEG concentration with large mobility values. Table 4 shows GaN epilayers grown on different substrates and their properties [36].

Table 4. GaN epilayers grown on different substrate properties [36].

	GaN	SiC	Sapphire	Si
κ, $W \cdot m^{-1} \cdot K^{-1}$ κ ($T^{-\eta}$)	150 $T^{-1.4}$	420 $T^{-1.3}$	35 T^{-1}	150 $T^{-1.3}$
TBR, $\times 10^{-8}\ W^{-1} \cdot m^2 \cdot K$				
Interface Temperature, °C		3.3 190	12 240	3.3 300

The developed power GaN HEMTs are increasingly entering the market and are well suited for high-power and high-voltage applications. This market is projected to achieve a significant performance improvement up to 100 times in comparison to Si [37]. GaN HEMTs for normally on and normally off architectures are commercially available in the voltage breakdown range of 200 to 650 V. GaN-based MOSFETs are still undergoing research and development, and different manufacturers have developed and commercialized SiO_2/GaN-interfaced MOSFETs and AlGaN/GaN-based MOS-HEMTs with high blocking voltage (2.5 kV) and high channel mobility values (170 cm^2/Vs). In 2010, International Rectifier announced their first GaN on silicon HEMT for high-power applications. This release was quickly followed by the launch of GaN devices in the range of 200 V by Efficient Power Conversion (EPC). The success of these devices was due to improvements in GaN-on-silicon epitaxy techniques [38]. This technique facilitated the creation of substrates with less impressive properties but at relatively low prices compared to GaN on SiC or GaN substrates. The price of the 4-inch silicon wafer was USD 100 for GaN epitaxy, while the 4-inch SiC wafer was at USD 130 and USD 7500 for the GaN wafer [39]. Figure 9 depicts the milestones and development of GaN power electronics devices throughout the past few years. The first GaN power devices were introduced during early 2010 to late 2011, where the first GaN power devices were released by International Rectifier, and since then, several successfully developed transistors have been reported, such as the GaN transistors (eGaN), 600 V GaN HEMTs, and 600 V GaN-on-SiC transistor. From early 2012 to mid-2014, the 6-inch GaN on Si was developed, whereas the 8-inch GaN on SiC was developed from mid-2014 to late 2016. Moreover, from 2018 to late 2019, the GaN system reached 150 A at 650 V [40].

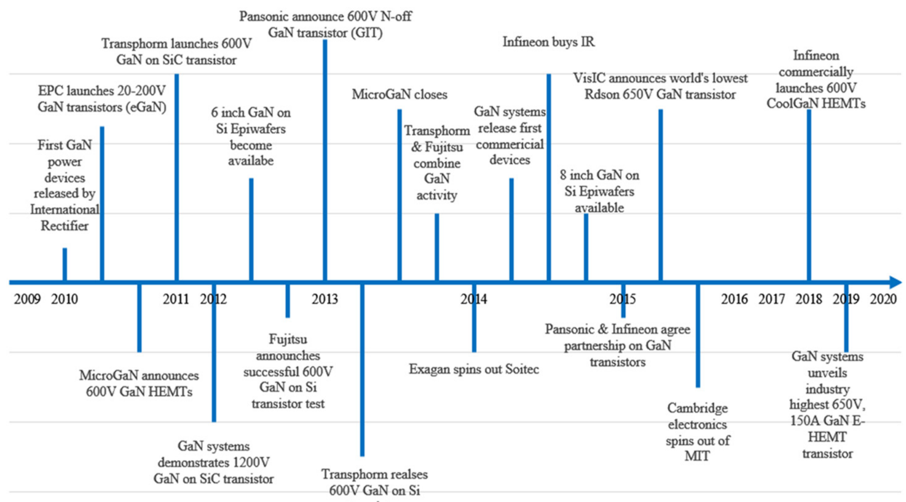

Figure 9. Milestones in GaN power electronics development.

The performance of GaN power devices has also improved since their introduction in 2010. Figure 10 illustrates the growth in current density from 2010 to 2012 and its predicted future trend up to 2020 [41]. Other GaN advancements include moving to larger 8-inch GaN-on-silicon wafers [42] and the introduction of gate injection transistors (GITs) in the power electronics market. GITs are tailor-made to perform well in the high-voltage range, with some of the devices rated up to 600 V. The major progress in GaN devices' research and development is attributed entirely to research labs and universities. The University of California Santa Barbara has been the leader in the development of high-quality GaN devices for power electronics [42].

Most companies involved in GaN devices are from the U.S. apart from MicroGaN and Infineon Technologies. Initially, Efficient Power Conversion (EPC), Transphorm, and MicroGaN were solely involved in the development of GaN power electronics devices. Now, other major companies such as Panasonic, Infineon, and Texas Instruments, who have been traditionally involved with Si-based devices, are also developing GaN devices. GaN power market was worth USD 126 million in 2021 and is expected to reach USD 6 billion by 2027 [43]. Table 5 shows GaN devices' development stage and the different product types upon which each company is focusing [44].

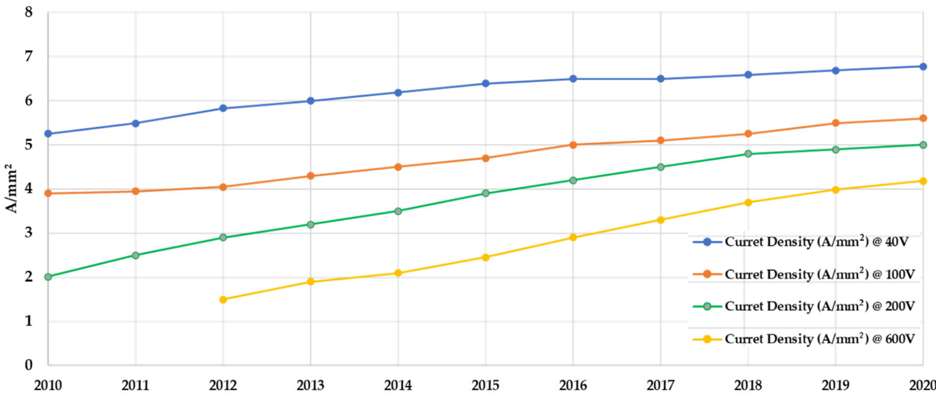

Figure 10. Current density trend for GaN [41].

Table 5. Development stages and product types for companies involved in GaN power electronics [44].

Vendor	Products		Technology	Development		Product Types		
	Open Market	**Closed Market**	**Foundry Services**	**Collaborative**	**In-House**	**Discrete**	**IC**	**Module**
IRF		✓				✓		✓
EPC	✓					✓		
Transphorm		✓						✓
Fujitsu					✓			
Sanken					✓		✓	
MicroGaN		✓	✓			✓		
Infineon					✓	✓		
HRL					✓	✓		
Panasonic					✓	✓	✓	
STM					✓	✓	✓	
RFMD		✓	✓			✓		
Toshiba					✓	✓		
GaN Systems					✓	✓		
NXP				✓		✓		
TI					✓	✓	✓	
Freescale					✓	✓	✓	
Powdec					✓	✓		
Renesas					✓	✓		
Furukawa					✓	✓		
POWI					✓		✓	
ON Semi				✓		✓	✓	
Intersil				✓	✓		✓	
Alpha & Omega					✓	✓		

2.3. Performance Advances in Diamond

Diamond's outstanding physical and electrical characteristics, which includes the highest known thermal conductivity, excellent electrical insulator properties, high breakdown voltage, and high carrier mobility, make it theoretically the best semiconductor for the next generation of power electronic devices [45]. Some of the potential applications include high-voltage power electronics, high-frequency high-power devices, and high-power optoelectronics devices, such as laser diodes and LEDs. During the last few years, diamond growth techniques have been significantly enhanced, and doping control methods for p, p+, n-type, and intrinsic diamond have been designed. Therefore, the electrical properties of diamond devices can now be characterized not just theoretically but also experimentally through device structures. Recently, planar diamond power Schottky barrier diode (SBD) test results reported a maximum breakdown field of 9.5 MV/m [46], blocking voltage of Vmax > 10 kV [47,48], high current operation above 20 A [49], and low switching losses with fast operation [50], making diamond SBDs an attractive material for power electronics applications. The first diamond-based power switching device was introduced in 1980s by Prins, using natural diamond crystals to form a bipolar junction transistor (BJT) with the usage of diamond crystals as the base electrode, while the n-type emitter and collector region were formed by carbon ion implantation [51]. However, due to device's geometrical issues associated with the fabrication process, the current gain was less than unity. Since then, other diamond-based power semiconductor devices such as metal-semiconductor FETs (MISFETs) [52] and metal-insulator-semiconductor FETs (MISFETs) were also designed using diamond crystals through ion implantation or diffusion doping. In the last decade, the situation has drastically changed with the introduction of various techniques of diamond epitaxial growth by chemical vapor deposition (CVD), high-pressure high-temperature (HPHT), microwave-enhanced chemical vapor deposition (MWCVD), and mosaic-type method. Producing high-quality defect-free wafers produced from diamond crystals is still a big challenge even with the application of different single-crystal growth techniques. With the HPHT technique, high-quality defect-free wafers of only few millimeters have been achieved so far, while for the SiC wafer. sizes up to 150 mm are available. The MWCVD and mosaic-type techniques are quite promising and are approaching wafer sizes of 2 inches, even though the defect density needs to be reduced in order to commercialize

the device on a large scale. Another interesting technique involves the heteroepitaxy of diamond on iridium, enabling the development of diamond films of up to 4 inches. Further development is required to reproduce controlled processes for manufacturing using this technique. Additionally, single-wafer material manufacturing for electronic applications is significantly impacted due to the difficulty of n-type doping with the lack of an efficient charge donor. Since p-type doping of naturally insulating diamond can easily be achieved by using boron, a great deal of development is being achieved on the fabrication of unipolar devices. Some of the CVD equipment makers for developing high-quality diamond wafers are shown in Figure 11 [53]. They can be broadly categorized into two groups based on method: hot filament chemical vapor deposition (HF CVD) and MW CVD.

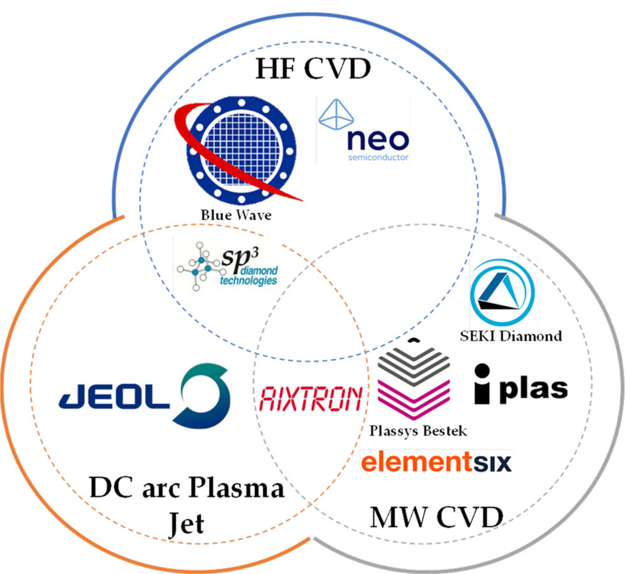

Figure 11. CVD equipment makers for development of high-quality diamond wafers.

2.4. Figure of Merit (FOM)

Various researchers have used numerous figures of merit (FOM) in order to evaluate different semiconductor materials performance. In 1965, Johnson [54] evaluated WBG semiconductor material for the first time and proposed an equation that could help identify possible future semiconductor materials. This author proposed that a semiconductor transistor performance can be evaluated using the critical breakdown field E_c and the electron drift velocity V_{sat} and came up with a FOM as $JM = (E_c V_{sat}/\pi)^2$. Later, Keyes [33] defined another FOM to evaluate semiconductors device performance as $KM = \lambda\sqrt{V_{sat}/\varepsilon}$, where λ is the thermal conductivity, and ε is the dielectric constant. In this FOM, power frequency for low-voltage transistors is also taken into account. When comparing these two FOMs, it becomes clear that saturation velocity and dielectric constant can be used on a broader level to evaluate some of the semiconductor devices. It is challenging, when evaluating a device's performance completely, to consider simultaneously the material's bandgap, thermal conductivity, and critical breakdown field.

To improve the efficiency and performance of semiconductor devices, it is essential to minimize power losses. Baliga [55] proposed the FOM, $BM = \varepsilon\mu E_c^3$, where μ represents the carrier mobility. This FOM helps reduce the conduction losses in power FETs. This FOM can only be evaluated for low frequencies, as it assumes that power losses are only due to current flowing through the on-resistance. To include higher-frequency switching losses, the author proposed another FOM, $BHFM = \mu E_c^2$, which assumes that losses occur when charging and discharging the input capacitance of FETs [56]. Another important factor contributing to power losses is the thermal conductivity. Shenai et al. defined three different thermal FOMs to incorporate various scenarios and factors. The first case scenario considers that if the thermal conductivity properties of heat sink material are different

compared to active device area, then the FOM is defined as QF1 = $\lambda\sigma$A. In the case of perfect heat sink material and with the assumption of an active device area at ambient temperature, the FOM can be defined as QF2 = $\lambda\sigma A E_c$. Finally, excluding any assumption related to heat sink material or geometry, the FOM can be defined as QF3 = σA. For all three cases, σA is equal to Baliga's FOM (i.e., $\varepsilon\mu E_c^3$) [57].

As more accurate data relating to new semiconductor materials properties became available, FOMs slowly evolved over time. Chow [58] discussed the problem with the assumption of the universal relationship between energy bandgap and breakdown voltage value when using Baliga's FOM for low frequencies. This universal relationship is not true for WBG semiconductors and hence cannot be effectively used to evaluate some devices. Baliga's FOM for higher frequencies is based on the assumption of linear relationship between energy bandgap and critical electric field, which is not true as well. Hence, there is a need for further investigation to develop new FOMs. Table 6 shows some FOMs normalized against Si, which were contributed from various researchers [59].

Table 6. FOMs contributed by various researchers [59].

Material	JM	KM	BM	BHFM	QF1	QF2	QF3
Si	1.00	1.00	1.00	1.00	1.00	1.00	1.00
Ge	-	-	0.13	0.28	0.05	0.02	0.13
Diamond (n)	5330	31	14,860	1080	198,100	5,784,410	14,860
Diamond (p)	6220	32	11,700	850	155,990	4,554,840	11,700
InP	13	0.72	10	6.6	26	38	10
InN ($\mu = 3000$)	58	6	46	19	150	460	46
InN ($\mu = 30,000$)	58	6	450	185	1500	4570	450
AlP	-	-	6.5	1.5	-	-	6.5
AIN ($\mu = 14$)	5120	2.6	390	14	660	25,520	390
AlN ($\mu = 1090$)	5120	2.6	31,670	1100	52,890	2,058,620	31,670
AlAs	630	-	7.3	2.0	-	-	7.3
AlSb	270	-	1.2	0.59	-	-	1.2
GaAs	11	0.45	28	16	9.4	16	28
GaN	790	1.8	910	100	910	10,300	910
GaP	37	0.73	16	3.8	9.4	41	16
BP	-	-		0.95	-	-	-
ZnSe	-	-	84	17	-	-	84
ZnS	-	-	94	17	-	-	94
ZnO	-	-	110	14	-	-	106
CdTe	-	-	5.3	3.0	-	-	5.3
CdSe	-	-	7.1	3.3	-	-	7.1
CdS	-	-	14	6.1	-	-	14
HgS	-	-	-	0.45	-		
6H-SiC	260	5.1	90	13	300	2440	90
3C-SiC	110	5.8	40	12	130	550	40
4H-SiC	410	5.1	290	34	950	9630	290
SnO_2	-	-	-	26	-	-	-
In_2O_3	-	-	-	1.8			

With the availability of new datasets for the critical electric field, Hudgins et al. [14] proposed a new derivation for the relationship between the critical electric field (ε_c, V/cm) and bandgap energy (EG, eV) for direct and indirect bandgap semiconductors and a new specific on-resistance (Ron_{sp}) to evaluate all semiconductor materials. The new generic relationship between critical electric field and bandgap energy is proposed as $\varepsilon_C = a(EG)^n$, where a is a prefactor fit parameter, and n is the exponent fit parameter. Table 7 shows values of a and n for direct, indirect, and for general semiconductor materials.

Table 7. Pre-factor fit (a) and exponent fit (n) parameters [14].

	a	n
All semiconductors	1.7485 × 105	2.359
Indirect bandgap only	2.3818 × 105	1.995
Direct bandgap only	1.7348 × 105	2.506

Using Table 7, the equation of the critical electric field for indirect semiconductors is $\varepsilon_C = 2.38 @ 105\ (EG)^2$, and for direct bandgap, $\varepsilon_C = 1.73 @ 105\ (EG)^{2.5}$.

Figures 12 and 13 show the original and new critical field equation difference for direct and indirect semiconductors.

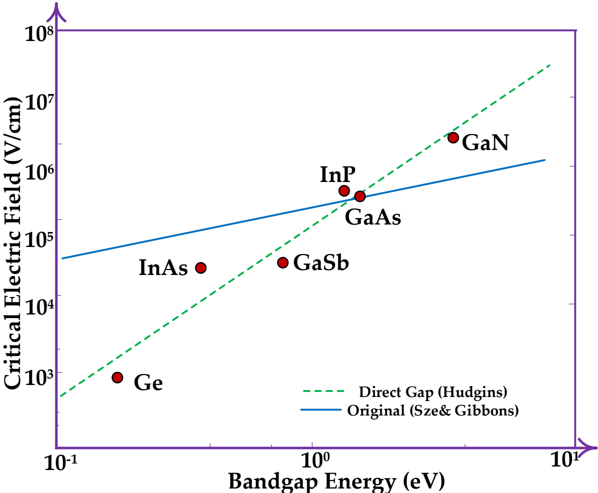

Figure 12. Direct bandgap semiconductors and new and old critical field difference [14].

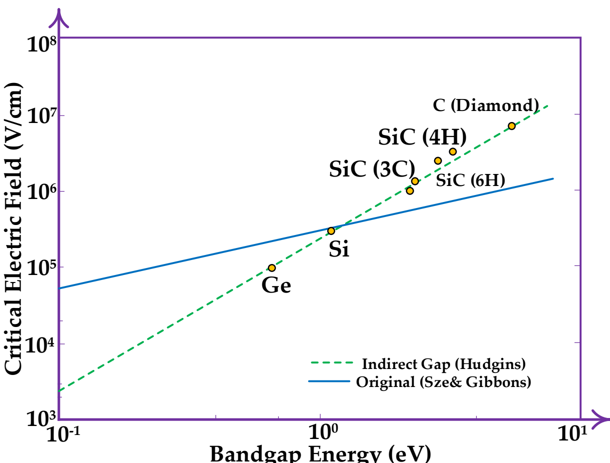

Figure 13. Indirect bandgap semiconductors and new and old critical field difference [14].

Specific on-resistance in terms of bandgap and voltage breakdown for indirect bandgap semiconductors was defined by Hudgins et al. [60] as follows:

$$Ron_{sp} = \frac{3.351 \times 10^{-3} V_B^2 (EG)^{-6}}{\mu_e\ \varepsilon_r} \quad \text{(Indirect)} \tag{1}$$

where Ron_{sp} is the specific on-resistance, V_B is the breakdown voltage, EG denotes the bandgap energy, μ_e is the electron mobility, and ε_r represents the relative permittivity. And for direct bandgap, the following is true:

$$Ron_{sp} = \frac{8.725 \times 10^{-3} V_B^2 (EG)^{-7.5}}{\mu_e\ \varepsilon_r} \quad \text{(Direct)} \tag{2}$$

Figure 14 shows the specific on-resistance for direct and indirect bandgap calculated using the new equations in comparison with old generic, specific on-resistance equation-based calculations.

Hence, Hudgins et al. proved that in the light of the new available data and derived equations, WBG semiconductors, especially GaN and SiC, are more favorable than previously thought [61].

Huang [62], on the other hand, proposed four new FOMs for different scenarios. If Ron and Q_{gd} are known, HDFOM can be used to evaluate different devices and is defined as HDFOM $= \sqrt{Ron{\cdot}Q_{gd}}$. HMFOM can be used to compare relative losses among the different devices and is defined as HFOM $= E_c\sqrt{\mu}$, while HCAFOM can be used to compare optimal chip area/size and is defined as HCAFOM $= \varepsilon\sqrt{\mu}E_c^2$. For the comparison of junction temperatures of different devices, HTFOM $= \sigma_{th}/\varepsilon E_c$ is employed. Table 8 shows a comparison of various semiconductor materials normalized against silicon, using the developed HMFOM, HCFOM, and HTFOM merits [10].

Table 8. Comparison of various semiconductor material using new FOMs (normalized against silicon) [10].

Semiconductor Material	Electron Mobility μ (cm^2/V-s)	Relative Dielectric Constant ϵ	Critical Field E_c (kV/cm)	Thermal Conductivity σ_{th} (W/m-K)	HMFOM $E_c\sqrt{\mu}$	HCFOM $\varepsilon\sqrt{\mu}E_c^2$	HTFOM $\sigma_{th}/\varepsilon E_c$
GaAs	8500	13.1	400	55	3.3	4.9	0.3
GaN	900	9	3000	110	8.	61.7	0.1
Ge	3900	16	100	58	0.6	0.3	1.0
Si	1400	11.7	300	130	1	1.0	1.0
GaP	250	11.1	1000	110	1.4	4.5	0.3
SiC (6H, α)	330	9.66	2400	700	3.9	25.7	0.8
SiC (4H, α)	1000	9.7	3180	700	7.5	65.9	0.8
Diamond	2200	5.7	5700	2000	23.8	220.5	1.7

Finally, Huang [10,63] concluded, using the new FOMs, that 4H-SiC will have 7.4 times lower losses compared to Si, a 65% smaller chip area, and 60% higher temperature. While GaN will have 8 times lower losses compared to Si, a 61.7% smaller area, and 10% higher temperature.

Based on the above FOMs, it is clear that GaN and SiC have better inherent properties, better efficiencies and can provide higher performance in comparison to current Si-based devices.

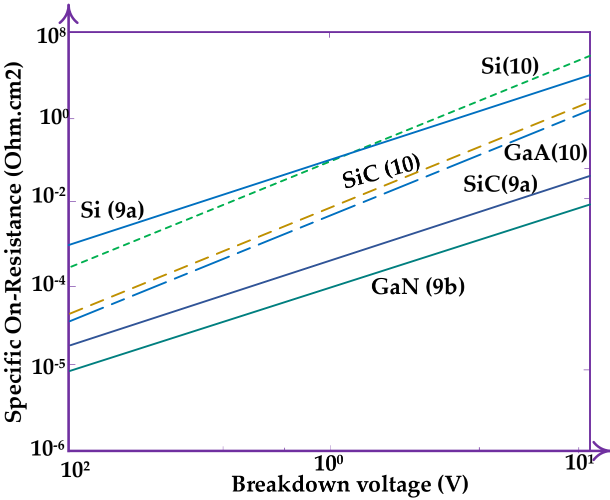

Figure 14. New on-resistance for direct bandgap shown as (9a) and new on-resistance for indirect bandgap as (9b), while (10) indicates on-resistance using old equation [14].

3. Applications

The initial successes of SiC and GaN devices in the market were at different ends of the voltage spectrum. SiC devices are preferred at voltage levels of 1200 V and above, while

GaN devices made inroads in applications with voltage ranges of up to 600 V and below. The two major reasons are the high switching speed and cost. GaN devices are smaller; hence, electrons require less time to travel through the device. Also, GaN crystals have higher and faster mobility of electrons. Therefore, for applications in the range of 600 V and below, GaN-based devices that can switch at faster speeds can provide better efficiency. SiC devices, on the other hand, are preferred for higher-voltage applications due to their size and maturity in device fabrication. For many high-power applications such as motor drives, uninterrupted power supply (UPS) systems, and high-voltage DC transmission systems (HVDC), a substantial size reduction can be achieved by using SiC devices. The usage of GaN, in-contrast to SiC devices, at a voltage level of 600 V and below is due to the cost-effective method of producing GaN. A GaN transistor can be grown on Si substrate wafers, while SiC requires expensive substrate. Furthermore, GaN low-voltage devices do not need expensive and bulky packages that are required for Si MOSFETs and SiC transistors [64]. However, with a better balance-of-plant system design, the total per-watt cost could potentially be reduced. These savings may result from the use of smaller passive inductive and capacitive circuit elements, filters, cooling, etc. These improvements could justify the higher capital cost in many power applications [65]. High-impact opportunities exist across a wide variety of applications, as discussed below.

3.1. Motor Drives

Electric motors are widely used in vast range of residential, commercial, and industrial applications, accounting for about 50% of the global energy consumption [66]. The global electric motor market is expected to grow from USD 134 billion in 2022 to USD 186 billion by 2027 [67]. The major portion of energy consumed in the residential sector is for cooling, heating, and refrigeration (fans and compressors). Similarly, in the commercial sector, most of the energy is consumed by HVAC and refrigeration. While, in the industrial sector, a vast portion of motor energy is consumed by conveyor systems, followed by compressor and pumps. Figure 15 illustrates the power consumption of electric motors in the residential and commercial sectors [68].

In the residential sector, low-power (0.75 to 4 kW) with low-input grid voltage (110 to 460 V) motors are currently used. In the commercial sector, both low-power and medium-power (4 kW to 375 kW) with medium-input voltage (200 V to 1000 V) motors are usually used. While, in the industrial sector, low-power, medium-power, and high-power (>375 kW) with high-input voltage (2.3 kV to 13.8 kV) motors are usually used depending on the application [69].

Variable frequency drives (VFDs) are commonly used to achieve variable speed. They consist of an input grid voltage rectifier and an inverter to adjust the voltage and frequency of the incoming current to meet the power requirements of the load. In centrifugal processes, such as fans and pumps, VFDs can save 55% less energy when running at 75% speed, based on the cubic relationship between the motor power and the speed [67]. On the other hand, in the case of applications requiring constant torque motors, e.g., conveyor belts, 25% energy is saved when running at 75% speed based on the linear relationship that exists between motor speed and power [70].

VFDs can reduce overall energy consumption by approximately 10–30% [67]. Globally, it is estimated that by employing VFDs, an energy saving of 10%, 15%, and 20%, respectively, for refrigeration, air compressor, and pumps/fan could be achieved [71]. Current Si-based VFDs have 10% market penetration with an average efficiency of 94.5%. Assuming an average saving of 15% with the adoption of VFDs for industrial electric motors, with 100% market penetration, the overall global energy losses in industrial motors are estimated at 214 TWh/year.

WBG devices are set to play a key role in improving the performance of current Si-based inverters for motor drives. Also, the current VFDs are quite bulky, require significant space due to cooling needs, and their efficiency should be improved for a wider adoption. WBG-based motor drives can run at higher frequencies, which can reduce the size of passive

components and reduce the audible system noise [72]. Additionally, WBG devices can withstand higher temperatures and thus can reduce the size and weight of the whole VFD, which is advantageous in many applications where space is a major constraint. The new generation of integrated motors drives (IMD) offers reduced weight, reduced volume, and higher efficiency. These motors drives are integrated inside a motor and can withstand high temperatures due to the superior physical characteristics of WBG-based power devices [73].

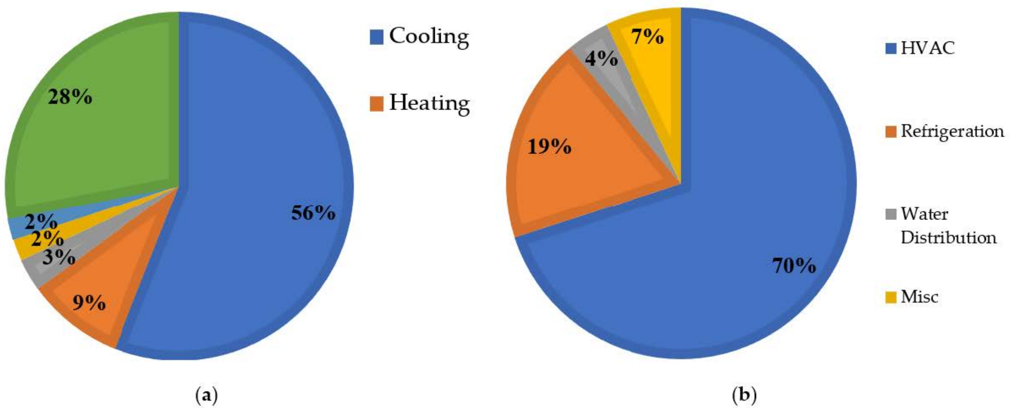

Figure 15. (**a**) Residential and (**b**) commercial motor electricity use [69].

Generally, low-power motors have higher variance in efficiency based on load requirements in comparison to larger motors. Therefore, as the VFD load decreases, so does the efficiency. The decrease in efficiency based on load is a problem and hinders the market penetration of VFDs, especially for lower-power motors. Motor losses were estimated at about 16 TWh globally in 2015 due to VFDs inefficiency. Figure 16 shows the efficiency of Si-VFD and WBG-based VFD against load fraction and rated power [73–76].

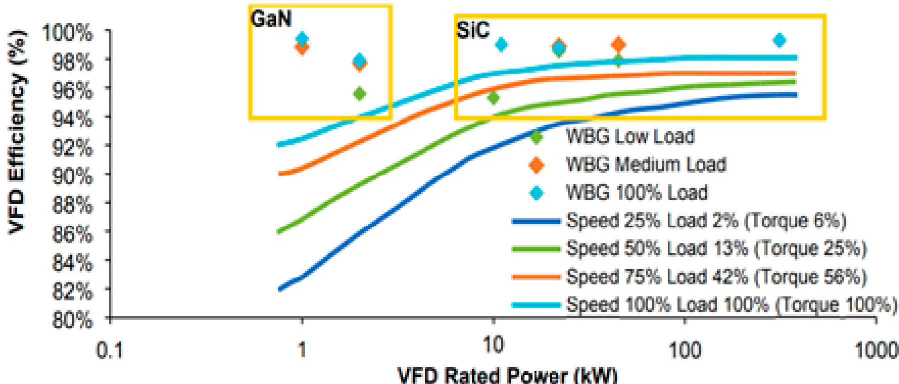

Figure 16. Electricity saving potential in industrial electric motors Si-based VFDs vs. WBG-based VFDs [74].

3.2. Automotive

WBG devices provide high power density with improved energy efficiency and are very promising for electrical vehicles (EVs) application. Some typical efficiency values of different converters are given in Table 9. Electric power train vehicles (H/EVs) can be classified into three types: battery electric vehicles (BEVs), hybrid electric vehicles (HEVs), and plug-in hybrid vehicles (PHEVs). In a BEV, the battery is primarily charged via an on-board charger (OBC) through standard 120 V or 240 V grid outlet. Regenerative braking can also contribute to charging when driving. Some of the leading BEVs include all models from Tesla, Nissan Leaf, and BMW i3. An HEV is comprised of a combustion engine, electric motor, generator, and a small battery. The battery can be charged by the combustion engine and via the generator during regenerative braking. HEVs are the most popular among all H/EVs [77].

Table 9. Efficiency of various converters in EVs.

Type	On-Board Charger	Inverters and HV Converter	Low-Voltage DC–DC Converter
Power	~3.3 kW	12–400 kW	1–10 kW
Input Voltage	120–240 V	200–400 V	200–400 V
Output Voltage	200–400 V	100–650 V	12–48 V
Si Efficiency	85–93%	83–95%	85–90%
SiC Efficiency	95–96%	96–97%	96–99%
GaN Efficiency	94–98%	No data	95–99%
Power Electronics	600–900 V	600 V–1.2 kV	600–900 V
	Discrete	Module and Discrete	Discrete
HEV	X	✓	✓
PHEV	✓	✓	✓
BEV	✓	✓	✓

Generally, electric drive systems in a typical EV consist of DC-DC buck/boost converter (mainly used in hybrid EVs) to step up the battery voltage up to 700 V, a traction inverter, a DC–DC converter for auxiliary loads, and an OBC.

1. The buck/boost converter requires high-voltage-rated devices typically in the range of 1.2 kV and a device for high switching frequencies in the order of tens of kilohertz (usually 100 kHz for a 20 kW buck/boost converter). Current SiC and GaN power devices can switch at higher frequencies without additional losses [12,78] and therefore are ideal candidates for this application. Operating these devices at higher frequencies can lower the overall footprint in terms of weight and size through a reduction in the output filter components, hence increasing the overall efficiency [79];
2. The traction inverter mainly requires lower switching and conduction losses and better thermal management. This makes SiC devices with a typical rating of 900 to 1.2 kV potential candidates for traction inverters. Also, the better thermal management of SiC devices translates into compact and lightweight heatsinks, which is necessary for traction inverters [80];
3. The DC–DC converter for handling auxiliary loads consists of both high-voltage interface and a low-voltage interface. For the high-voltage side, SiC is the best candidate, while for low voltages, GaN devices can easily fulfill the requirements. Also, the DC–DC converter typically requires higher-frequency operation (to decrease the size of the output filter components), which the current WBG devices can easily achieve without creating additional switching losses [81];
4. The present OBCs are currently designed for wired operation, while the future tendency is for the wireless charging. Furthermore, OBCs operate more efficiently with high-frequency switching devices. Toyota and APEI have developed a 6 kW SiC OBC system operating at switching frequencies up to 250 kHz, with an overall efficiency of 95% and 10 times improvement in power density [82]. Also, a SiC-based OBC of 6.8 kW demonstrated 50% reduction in component count and 2% increase in efficiency [83].

In an EV, energy efficiency can be achieved directly through the reduction of switching and other losses and indirectly by reducing the volume and weight of power electronics circuitry. The EV Everywhere Grand Challenge launched in the U.S. in 2013 required 35% reduction in size and 40% reduction in weight, which can be achieved by WBG devices, especially SiC [84]. Estimates of drive efficiencies can be determined by comparing Si and SiC drive performance over a range of speed and torque. Table 10 illustrates Si and SiC inverter efficiency over different drive cycles [85,86].

Table 10. Inverter efficiency of Si and SiC over various drive cycles [85,86].

Drive Cycle	Type	Si	SiC	Improvement	Reduction of Losses
US06	Aggressive	95.1%	97.1%	2.1%	41%
EPA City	City	90.9%	97.9%	7.7%	77%
EPA Highway	Highway	97.7%	99.7%	2.0%	85%
Artemis Urban	City	86.2%	96.6%	12%	76%
Empa C1	City	82.9%	96.0%	16%	77%
Hyzem Urban	City	87.2%	96.7%	11%	75%

As the price of SiC and GaN devices drops, more manufacturers in the automotive industry are adopting them. Toyota has already announced the introduction of the SiC-based power control unit (PCU) for EVs by 2020 [87]. While other automotive makers like Ford Motors have recently demonstrated a 40% reduction in switching losses and an overall fuel efficiency of 5% by adopting SiC MOSFETs [88]. It is expected that by adopting SiC MOSFETs in hybrid EVs, an improvement of up to 15% could be achieved, and significant savings could also be made by drivetrain electrification [56]. In addition, WBG-based converters enable efficient, lightweight, and low-cost DC charging infrastructure (>120 kW), which, coupled with cleaner electricity generation in the transportation sector, can potentially reduce greenhouse gas emissions [89].

3.3. Data Centers

A data center consists of networked computers servers that are utilized for data processing, storage, and distribution. These servers are responsible of providing local intranets, data clouds, and Internet. Approximately, 2.5 billion people around the world are online now, with millions of searches, emails, and online transactions routed via these centers each minute [90]. As these numbers are increasing each year, data centers' efficiency has become quite critical. A major concern is the high electricity usage in the data center industry due to lack of motivation to improve the equipment efficiency. Figure 17 below shows global energy usage in data centers [91].

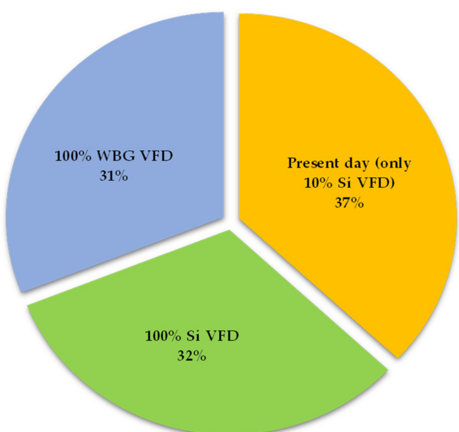

Figure 17. Electricity-saving potential in industrial electric motors Si-based VFDs vs. WBG-based VFDs [44].

The increase in global data center electricity usage has led many governments across the world to introduce regulations and efficiency standards for data centers. Energy usage in a modern data center includes mainly the IT load, UPS and cooling systems. The IT load consumes approximately half of the energy of a data center and consists of the servers, data storage, power supply unit (PSU), and network devices. The rest is utilized for additional power conversion involving UPS, transformers, and cooling units. Figure 18 below illustrates the energy usage breakdown of a data center [92].

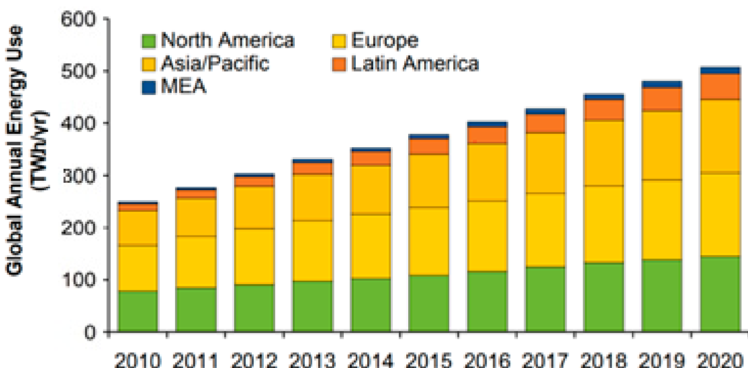

Figure 18. Global energy usage in data centers.

The power system of a data center consists of a line frequency transformer, low-voltage power distribution network, and centralized backup unit voltage regulators. Typically, the power conversion tasks involved in an average data center account for 10.4% of the total energy consumed [93] There are several factors for the high-power usage of a data center, such as the underutilization of servers and UPS units that are on but not fully utilized and inefficient cooling solutions.

Different energy efficiency improvement schemes range from the adoption of low-power losses converters to a complete redesign of the power delivery network. The latter would likely involve converting higher voltages at the rack level, where space is limited, and require an efficient thermal management. WBG-based converters can play a key role in the development of efficient systems by reducing the impact of higher temperatures on the loads without incorporating expensive and bulky cooling solutions.

In a data center, power conversion equipment based on standard silicon devices such as rectifier, inverter, and converter are approximately 75 to 95% efficient [94]. Among the power conversion equipment are UPS and PSU systems.

A UPS unit is critical part of any data center, as it provides backup power to the load in case of electricity outage. The UPS employs a double-conversion strategy: during normal operation, the AC grid voltage is rectified into DC and then stored in a battery, while during grid failure, the inverter converts the stored DC voltage back into AC. Though this ensures a continuous supply of power, it ultimately generates significant losses during the conversion of AC–DC–AC [95]. SiC-based UPS are now commercially available from well-known manufacturers such as Toshiba and Mitsubishi. The G2020 UPS unit from Toshiba boasts half the losses, has a higher operating temperature, is compact in size, and is only 10% more expensive compared to a similarly sized silicon-based UPS system [96].

The PSU used in servers converts AC power from the power distribution unit (PDU) into low-voltage DC. It consists of an AC-to-DC rectifier, a step-down transformer, and a DC–DC converter. For most data centers, the input AC supply voltage to the PSU ranges from 200 V to 480 V, while the output voltage is typically 12 V DC. WBG power devices such as SiC are commercially available in the range of 600 V to 1.2 kV, while for GaN, the voltage is up to 600 V. These power devices can easily replace the existing silicon devices [97]. Similarly to the UPS systems, it is estimated that replacing the standard silicon power devices such as diodes and transistors with WBG can reduce the power losses by half [98]. In a study, GaN-based PSU for data centers demonstrated an efficiency of 96.3% at a switching frequency of 1MHz. This led to a reduction in the converter size, transformer winding losses, and heat produced by the converter. Figure 19 below shows energy usage of data center equipment based on Si and WBG devices [99].

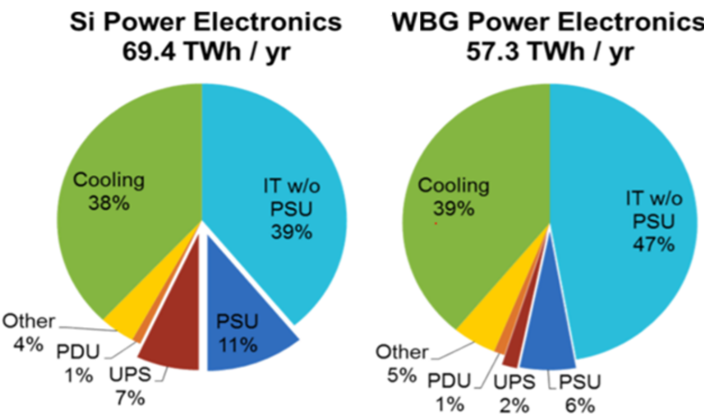

Figure 19. Data center electricity usage of Si and SiC equipment.

Switching from Si-based devices to WBG-based devices can increase the energy conversion efficiency from 90% to 98% in data centers [100]. This translates into an approximately 8.3% reduction in energy usage. In addition to the energy savings, due to low-power losses, the WBG-based data center equipment can operate at higher temperatures without requiring expensive and bulky cooling solutions.

3.4. Power Systems and Distributed Energy Resources

Power electronics technology is already playing an essential role in electric power systems applications, such flexible alternating current transmissions systems (FACTS), high-voltage direct current (HVDC) transmission, and the integration of distributed renewable energy sources such as solar photovoltaics (PV) and wind energy into the power grid. Renewable energy resources vary from other traditional power generation sources (coal, oil, etc.) since the voltage is usually converted from DC to AC to supply power suitable for grid integration. The rapidly growing penetration of renewable energy resources has increased the opportunity for WBG devices. It is estimated that about 4% of all the electricity generated is lost in the power electronics devices [101].

In 2014, the U.S. alone generated 77 TBtu of energy from solar PV [102]. The energy savings when switching from Si- to SiC-based inverters are expected to increase from 96% to 99%, i.e., a 3% increase [103]. Additionally, WBG devices offer an increase in the system-level efficiency by operating PV systems at higher voltages. This reduces voltage conversions in a traditional PV converter by replacing the combiner boxes with DC–DC converters.

On the other hand, modern wind turbines generate variable AC power, which depends on wind speed. The variable frequency AC power needs to be rectified into DC and then back into AC to achieve a fixed grid frequency. Though the conversion process has a set of associated losses, it allows wind turbines to function at maximum efficiency. In 2014, approximately 572 TBtu of energy in the U.S. was produced through wind turbines [104]. An improvement from 93.5% to 97.8% with absolute 4.6% efficiency is possible by incorporating WBG devices for wind energy conversion systems [105]. A 100% penetration of SiC devices in the wind turbine converters industry is expected to generate an annual savings of 26.3 TBtu. WBG devices offer low system-level costs by operating at higher switching frequencies, which in turn reduces the size of passive components and overall system footprint. Also, WBG devices-based converters are robust and have a mean time to failure (MTTF) of more than 25 years [106]. This lowers the operation and maintenance of the equipment and thus the overall cost of the system in a distributed energy resources (DERs) application.

3.5. Consumer Electronics

In 2019, the International Energy Agency (IEA) reported that 1.7% of the global energy consumption, estimated at 50 TWh, consists of external power supplies (EPS) such as laptops and mobile phones [107]. It is estimated that 45% of this energy (23 TWh)

is dissipated in mobile phones, MP3, and AC adapters. This includes losses between electronic devices and AC sources. Various assumptions are made when estimating the energy usage of AC adapters and external power supplies (EPSs). A U.S. Department of Energy (DOE) study broadly identified four states of EPS modes—active, no-load, off, and unplugged, depending on its connection to the power source and the application and state of EPSs on/off switch. The active mode can be further classified into six states ranging from 66% of EPS power, in the case of the computer just being turned on, to a 0.6% output power, when the computer is fully charged and switched off [108].

GaN HEMTs are an ideal candidate for electronic device adapters, especially for laptops, and could increase the efficiency by 3%. This is a conservative estimate, as laptop adapters usually offer a partial percentage of their rated power, and GaN HEMTs truly shine at lower levels. Table 11 illustrates the benefits of switching to WBG-devices-based adapters for laptops, mobile phones, and tablets [97]. An increase of 3% in the efficiency for laptops, 5% for mobile phones, and 9% for tablets should translate into an overall annual saving of 7670 GWh for the U.S. alone, which approximates the annual generation of an average-sized coal power plant. Another important benefit of using high-frequency GaN devices is a 10 times reduction in an average adapter size. Consumers would willingly pay a higher cost towards a more compact adaptor size based on GaN devices, which in turn will help drive the sales volume and achieve comparable cost reductions. In the future, when GaN power devices eventually reach a reasonable price, their introduction in flatscreen TV power supplies and various other consumer electronics will substantially increase.

Table 11. Potential impact of WBG components on global energy.

Transistor Material	Application	Average Power Rating (W) (1)	Average Active Mode Efficiency (1)	Annual Loss per Unit (kWh)	2014 Global Sales (2)	Assumed Product Life (Years) (3)	Global Stock (MM Units in Service)	Annual Electricity Loss by Global Stock (GWh)
	Laptop	60	87%	11.0	250	3	750	8250
Si	Tablet	12	80%	1.9	250	3	750	1425
	Cell phone	5	63%	4.2	1870	3	5610	23,562
				Total				33,237
	Laptop	60	90%		250	3	750	6346
WBG	Tablet	12	85%	1.5	250	3	750	1096
	Cell phone	5	72%	3.2	1870	3	5610	18,125
				Total				25,567
				WBG Savings (GWh/year)				7670
				WBG Savings (GWh/year)				26.2

4. Challenges Facing WBG Devices

Despite exceptional headways in WBG semiconductors, significant work still needs to be done before the full potential of these materials is realized. As discussed above, essential research into material properties and processing, with improvement down the power electronics value chain into circuits and systems, represents a crucial stride in the development of these unique materials in order to receive the energy benefits through far-reaching applications. The current challenges preventing the widespread adoption of WBG devices are summarized below.

Maturity and reliability—WBG semiconductors and devices are relatively less mature than Si-based conventional counterparts. There is also a limited availability of WBG devices in the market due to the large demand-to-supply ratio.

Heat dissipation—While WBG materials can handle higher temperatures than silicon, they can still generate significant heat, especially in high-power applications.

Lack of standardization—WBG technologies are still developing, and there is a lack of standardization compared to Si-based conventional counterparts. This can result in compatibility issues and slower adoption in some industries.

Higher switching frequencies—Electromagnetic interference (EMI) and electromagnetic compatibility (EMC) compliance is a challenge during higher switching frequencies operation.

Cost and quality—WBG material is very costly to manufacture due the high cost of SiC and GaN substrates and the difficulty to produce high-quality wafers with limited crystalline defects as compared to similarly rated Si-based devices.

Device design and fabrication—Novel design techniques are needed to realize the full potential of WBG devices properties to achieve the voltage and current requirements in various applications. Also, advanced device packaging and thermal management technologies need to be developed to improve operating temperatures, architectures, and manufacturing affordability for wide-scale adoption of WBG devices.

Systems integration—In many applications, simple drop-in replacement of Si with WBG devices is not always appropriate due to the significant differences in material properties. Therefore, for large and more complex systems, circuits must be redesigned for effective integration of WBG devices to utilize their full capability.

5. Conclusions

Even though WBG devices are rapidly gaining acceptance, there are risks and anxiety associated with the increased research and investment in WBG materials. There are concerns of losing intellectual property of WBG devices to countries like China that have large capabilities for semiconductors production facilities. Additionally, serious concerns regard the cost of WBG materials, from the possibility of never becoming lower or the reliability of WBG devices for large-scale adoption in various applications. Risks and uncertainties regarding the manufacturing cost of WBG devices can be broken down to three major categories.

Finally, external factors such as lenient efficiency standards in emerging markets and falling electricity prices due to the increased deployment of renewable energy power generation might deter businesses from using high-efficiency power electronics due to the long-term payback period. To alleviate some concerns regarding the reliability of WBG devices, leading manufacturers Cree and GE recently released data showing marked improvements with each iteration of their devices. Also, it is expected that the cost of WBG devices will eventually reach price parity with current silicon devices (10 cent/A) in the next five years through the usage of commercial silicon foundries and may fall even below the current price (1.5 cent/A) through the introduction of a fine-line lithography technique made possible by flatter wafers. With the introduction of 8-inch SiC wafers in 8 years' time, prices could fall even lower (1 cent/A for 1200 V devices).

Funding: This research received no external funding.

Data Availability Statement: Not applicable.

Conflicts of Interest: The authors declare no conflict of interest.

References

1. Kizilyalli, J.C.; Xu, Y.A.; Carlson, E.; Manser, J.; Cunningham, D.W. Current and future directions in power electronic devices and circuits based on wide band-gap semiconductors. In Proceedings of the 2017 IEEE 5th Workshop on Wide Bandgap Power Devices and Applications (WiPDA), Albuquerque, NM, USA, 30 October–1 November 2017; p. 417.
2. Millan, J.; Godignon, P.; Perpina, X.; Perez-Tomas, A.; Rebollo, J. A Survey of Wide Bandgap Power Semiconductor Devices. *IEEE Trans. Power Electron.* **2014**, *29*, 2155–2163. [CrossRef]
3. Saeed, H.T.R.; Kurdkandi, N.V.; Husev, O.; Vinnikov, D.; Tahami, F. An overview of lifetime management of power electronic converters. *IEEE Access* **2022**, *10*, 109688–109711.
4. Elasser, A.; Chow, T. Silicon carbide benefits and advantages for power electronics circuits and systems. *Proc. IEEE* **2002**, *90*, 969–986. [CrossRef]
5. Shenai, K. Potential impact of emerging semiconductor technologies on advanced power electronic systems. *IEEE Electron. Device Lett.* **1990**, *11*, 520–522. [CrossRef]
6. Langpoklakpam, C.; Liu, A.-C.; Chu, K.-H.; Hsu, L.-H.; Lee, W.-C.; Chen, S.-C.; Sun, C.-W.; Shih, M.-H.; Lee, K.-Y.; Kuo, H.-C. Review of silicon carbide processing for power MOSFET. *Crystals* **2022**, *12*, 245. [CrossRef]

7. Carlson, E.P.; Kizilyalli, I.C.; Cunningham, D.W.; Manser, J.S.; Xu, Y.A.; Liu, A.Y. *Wide Band-Gap Semiconductor-Based Power Electronics for Energy Efficiency*; Advanced Research Projects Agency-Energy, US Department of Energy (USDOE): Washington, DC, USA, 2018.
8. Schafer, R.; Buchalter, J. *Semiconductors: Technology and Market Primer 10.0*; Oppenheimer & Co.: New York, NY, USA, 2017.
9. Tuztasi, F.M.; Aydin, M. The Effect of Temperature Changes on Semiconductor Material Efficiency Under Load. In Proceedings of the 2022 11th International Conference on Renewable Energy Research and Application (ICRERA), Istanbul, Turkey, 18–21 September 2022; IEEE: Piscataway, NJ, USA, 2022; pp. 496–501.
10. Ballestín-Fuertes, J.; Muñoz-Cruzado-Alba, J.; Sanz-Osorio, J.F.; Laporta-Puyal, E. Role of wide bandgap materials in power electronics for smart grids applications. *Electronics* **2021**, *10*, 677. [CrossRef]
11. Neudeck, P.G.; Okojie, R.S.; Chen, L.-Y. High-temperature electronics—A role for wide bandgap semiconductors? *Proc. IEEE* **2002**, *90*, 1065–1076. [CrossRef]
12. Armstrong, K.O.; Das, S.; Cresko, J. Wide bandgap semiconductor opportunities in power electronics. In Proceedings of the 2016 IEEE 4th Workshop on Wide Bandgap Power Devices and Applications (WiPDA), Fayetteville, AR, USA, 7–9 November 2016; IEEE: Piscataway, NJ, USA, 2016; pp. 259–264.
13. California Energy Commision. *Go Solar California Project. List of Eligible Inverters per SB1 Guidelines*; California Energy Commission: Sacramento, CA, USA, 2016.
14. Hudgins, J.; Simin, G.; Santi, E.; Khan, M. An assessment of wide bandgap semiconductors for power devices. *IEEE Trans. Power Electron.* **2003**, *18*, 907–914. [CrossRef]
15. White House. Press Release: President Obama Announces New Public-Private Manufacturing Innovation Institute. 2014. Available online: https://www.presidency.ucsb.edu/documents/fact-sheet-president-obama-announces-new-manufacturing-innovation-institute-competition (accessed on 26 July 2023).
16. Semiconductor Sales Worldwide from 2015 to 2022, by Region. Available online: https://www.statista.com/statistics/249509/forecast-of-semiconductor-revenue-in-the-americas-since-2006/ (accessed on 26 July 2023).
17. Eden, R. *The World Market for Silicon Carbide & Gallium Nitride Power Semiconductors*; IHS Technology: London, UK, 2016.
18. Nalwa, H.S. (Ed.) *Handbook of Surfaces and Interfaces of Materials*; Five-Volume Set; Elsevier: Amsterdam, The Netherlands, 2001.
19. Stęszewski, J.; Jakubowski, A. Comparison of 4H-SiC and 6H-SiC MOSFET I-V characteristics simulated with Silvaco Atlas and Crosslight Apsys. *J. Telecommun. Inf. Technol.* **2007**, *3*, 93–95.
20. Singh, R. Reliability and performance limitations in SiC power devices. *Microelectron. Reliab.* **2006**, *46*, 713–730. [CrossRef]
21. Casady, J.B. SiC power devices and modules maturing rapidly. *Power Electron. Eur.* **2013**, *1*, 16–19.
22. Cree Inc. Milestones. About Cree. From 580. 2014. Available online: http://www.cree.com/About-Cree/History-and-Milestones/Milestones (accessed on 28 October 2014).
23. Hiroaki, F.; Ito, M.; Ito, H.; Kamata, I.; Naito, M.; Hara, K.; Yamauchi, S.; Suzuki, K.; Yajima, M.; Mitani, S. Development of a 150 mm 4H-SiC epitaxial reactor with high-speed wafer rotation. *Appl. Phys. Express* **2013**, *7*, 015502.
24. Xu, Y.A. *ARPA-E Impacts: A Sampling of Project Outcomes*; Advanced Research Projects Agency-Energy (ARPA-E), US Department of Energy (USDOE): Washington, DC, USA, 2018; Volume III.
25. JCN Newswire. SDK Increases Capacity to Produce 6″ SiC Epi-Wafers for Power Devices. Sys-con Media. 2014. Available online: http://www.sys-con.com/node/3192617 (accessed on 28 October 2014).
26. Hull, B. SiC Power Devices—Fundamentals, MOSFETs and High Voltage Devices. In Proceedings of the 1st IEEE Workshop on Wide Bandgap Power Devices and Applications, Columbus, OH, USA, 27–29 October 2013; IEEE: Piscataway, NJ, USA, 2013.
27. Seal, S.; Mantooth, H.A. High performance silicon carbide power packaging—Past trends, present practices, and future directions. *Energies* **2017**, *10*, 341. [CrossRef]
28. Department of Energy. Wide Bandgap Power Electronics Technology Assessment. Available online: https://www.energy.gov/sites/prod/files/2015/02/f19/QTR%20Ch8%20-%20Wide%20Bandgap%20TA%20Feb-13-2015.pdf (accessed on 28 October 2014).
29. Maddi, H.L.R.; Yu, S.; Zhu, S.; Liu, T.; Shi, L.; Kang, M.; Xing, D.; Nayak, S.; White, M.H.; Agarwal, A.K. The road to a robust and affordable SiC power MOSFET technology. *Energies* **2021**, *14*, 8283. [CrossRef]
30. Yole Développement. *Status of the Power Electronics Industry: A Comprehensive Overview of the Power Electronics Semiconductors Business*; Yole Développement: Rhone-Alpes, France, 2012.
31. O'Loughlin, M.; Burk, A.; Tsvetkov, D.; Ustin, S.; Palmour, J.W. Advances in 3x150 mm Hot-Wall and 6x150 mm Warm-Wall SiC Epitaxy for 10kV-Class Power Devices. *Mater. Sci. Forum* **2016**, *858*, 167–172. [CrossRef]
32. Zolper, J.C. Emerging silicon carbide power electronics components. In Proceedings of the Twentieth Annual IEEE Applied Power Electronics Conference and Exposition, Austin, TX, USA, 6–10 March 2005; IEEE: Piscataway, NJ, USA, 2005; Volume 1, pp. 11–17. [CrossRef]
33. Yole Développement. *Power SiC 2018: Materials, Devices and Applications by the Power & Wireless Team at Market Research and Strategy Consulting Company*; Yole Développement: Rhone-Alpes, France, 2018.
34. Friedrichs, P. Further Prospects with SiC power semiconductors—Schottky diodes, JFET transistors and package considerations. In Proceedings of the 1st IEEE Workshop on Wide Bandgap Power Devices and Applications, Columbus, OH, USA, 27–29 October 2013; IEEE: Piscataway, NJ, USA, 2013.
35. Roussel, P. All Change for Silicon Carbide. Compound Semiconductor. 2013. Available online: http://www.compoundsemiconductor.net/article/90863-all-change-for-silicon-carbide.html (accessed on 28 October 2014).

36. Green Car Congress. Toyota Beginning On-Road Testing of New SiC Power Semiconductor Technology; Hybrid Camry Fuel Cell Bus. 29 January. Available online: http://www.greencarcongress.com/2015/01/20150129-toyotasic.html (accessed on 28 October 2014).
37. Chernykh, M.Y.; Andreev, A.A.; Ezubchenko, I.S.; Chernykh, I.A.; Mayboroda, I.O.; Kolobkova, E.M.; Khrapovitskaya, V.; Grishchenko, J.V.; Perminov, P.A.; Sedov, V.S.; et al. GaN-based heterostructures with CVD diamond heat sinks: A new fabrication ap-proach towards efficient electronic devices. *Appl. Mater. Today* **2022**, *26*, 101338. [CrossRef]
38. Yaozong, Z.; Zhang, J.; Wu, S.; Jia, L.; Yang, X.; Liu, Y.; Zhang, Y.; Sun, Q. A review on the GaN-on-Si power electronic devices. *Fundam. Res.* **2022**, *2*, 462–475.
39. Sarua, A.; Ji, H.; Hilton, K.; Wallis, D.; Uren, M.; Martin, T.; Kuball, M. Thermal Boundary Resistance Between GaN and Substrate in AlGaN/GaN Electronic Devices. *IEEE Trans. Electron Devices* **2007**, *54*, 3152–3158. [CrossRef]
40. Yole Developpement. A comprehensive overview of the 680 power electronics semiconductors business. In *Status of the Power Electronics Industry*; Yole Developpement: Villeurbanne, France, 2012.
41. Würfl, J.; Hilt, O. *Power Electronic Devices Based on GaN: Advantages and Perspectives*; Societe des Ingenieurs de l'Automobile (SIA): SURESNES CEDEX, France, 2013; Available online: https://www.sia.fr/publications/241-power-electronic-devices-based-on-gan-advantages-and-perspectives?lng=en (accessed on 23 June 2019).
42. Ravkowski, J.; Peftitsis, D.; Nee, H.-P. Recent Advances in Power Semiconductor Technology. In *Power Electronics for Renewable Energy Systems, Transportation and Industrial Applications*; Abu-Rub, H., Malinowski, M., Al-Haddad, K., Eds.; John Wiley & Sons, Ltd: Chichester, UK, 2014. [CrossRef]
43. Yolegroup. Power GaN Supply Chain. 2018. Available online: https://www.yolegroup.com/Power_GaN_SupplyChain_HEMTcomparison.aspx (accessed on 23 June 2019).
44. ORNL. *Oak Ridge National Lab Wide Band Gap Device Suppliers Survey*; ORNL: Oak Ridge, TN, USA, 2013.
45. Diel, Z. Commercial Status of the GaN-on-Silicon Power Industry. Compound Semiconductor. 11–15 March 2013. Available online: http://venture-q.com/pdf/Venture-QArticle-Web.03.05.13.pdf (accessed on 28 October 2014).
46. Umezawa, H. Recent advances in diamond power semiconductor devices. *Mater. Sci. Semicond. Process.* **2018**, *78*, 147–156. [CrossRef]
47. Volpe, P.-N.; Muret, P.; Pernot, J.; Omnès, F.; Teraji, T.; Jomard, F.; Planson, D.; Brosselard, P.; Dheilly, N.; Vergne, B.; et al. High breakdown voltage Schottky diodes synthesized on p-type CVD diamond layer. *Phys. Status. Solidi A* **2010**, *207*, 2088–2092. [CrossRef]
48. Volpe, P.-N.; Muret, P.; Pernot, J.; Omnès, F.; Teraji, T.; Koide, Y.; Jomard, F.; Planson, D.; Brosselard, P.; Dheilly, N.; et al. Extreme dielectric strength in boron doped homoepitaxial diamond. *Appl. Phys. Lett.* **2010**, *97*, 223501. [CrossRef]
49. Suzuki, M. High voltage diamond pin diodes: Feasibility study on ultimate properties of diamond toward ultimate power devices. *Oyo Buturi* **2016**, *85*, 218–222.
50. Bormashov, V.S.; Terentiev, S.A.; Buga, S.G.; Tarelkin, S.A.; Volkov, A.P.; Teteruk, D.V.; Kornilov, N.V.; Kuznetsov, M.S.; Blank, V.D. Thin large area vertical Schottky barrier diamond diodes with low on-resistance made by ion-beam assisted lift-off technique. *Diam. Relat. Mater.* **2017**, *75*, 78–84. [CrossRef]
51. Umezawa, H.; Shikata, S.; Funaki, T. Diamond Schottky barrier diode for high-temperature, high-power, and fast switching applications. *Jpn. J. Appl. Phys.* **2014**, *53*, 05fp06. [CrossRef]
52. Prins, J.F. Bipolar-transistor action in ion-implanted diamond. *Appl. Phys. Lett.* **1982**, *41*, 950–952. [CrossRef]
53. Zeisse, C.R.; Hewett, C.A.; Nguyen, R.; Zeidler, J.R.; Wilson, R.G. An ion-implanted diamond metal-insulator semiconductor field-effect transistor. *IEEE Electron Device Lett.* **1991**, *12*, 602–604. [CrossRef]
54. Yole Developpement. *Diamond Materials for Semiconductor Applications*; Yole Developpement: Villeurbanne, France, 2013.
55. Keyes, R.W. Figure of Merit for Semiconductors for High-Speed Switches. *Proc. IEEE* **1972**, *60*, 225–232. [CrossRef]
56. Baliga, B.J. Power Semiconductor Device Figure of Merit for High-Frequency Applications. *IEEE Electron Device Lett.* **1989**, *10*, 455–457. [CrossRef]
57. Ozpineci, B.; Tolbert, L. Comparison of Wide-Bandgap Semiconductors for Power Electronics Applications. Master's Thesis, U.S. Department of Energy, Washington, DC, USA, 2003.
58. Werner, M.; Fahrner, W. Review on materials, microsensors, systems and devices for high-temperature and harsh-environment applications. *IEEE Trans. Ind. Electron.* **2001**, *48*, 249–257. [CrossRef]
59. Chow, T.; Tyagi, R. Wide bandgap compound semiconductors for superior high-voltage unipolar power devices. *IEEE Trans. Electron Devices* **1994**, *41*, 1481–1483. [CrossRef]
60. Oleksiy, S.; Flicker, J.; Dickerson, J.; Shoemaker, J.; Binder, A.; Smith, T.; Goodnick, S.; Kaplar, R.; Hollis, M. Analysis of the dependence of critical electric field on semiconductor bandgap. *J. Mater. Res.* **2022**, *37*, 849–865.
61. Tsao, J.Y.; Chowdhury, S.; Hollis, M.A.; Jena, D.; Johnson, N.M.; Jones, K.A.; Kaplar, R.J.; Rajan, S.; Van de Walle, C.G.; Bellotti, E.; et al. Ultrawide-bandgap semiconductors: Research opportunities and challenges. *Adv. Electron. Mater.* **2018**, *4*, 1600501. [CrossRef]
62. Shenai, K.; Scott, R.; Baliga, B. Optimum semiconductors for high-power electronics. *IEEE Trans. Electron Devices* **1989**, *36*, 1811–1823. [CrossRef]
63. Zhang, L.; Zheng, Z.; Lou, X. A review of WBG and Si devices hybrid applications. *Chin. J. Electr. Eng.* **2021**, *7*, 1–20. [CrossRef]
64. Huang, A. New Unipolar Switching Power Device Figures of Merit. *IEEE Electron Device Lett.* **2004**, *25*, 298–301. [CrossRef]

65. Epc-co.com. Efficient Power Conversion Corporation. 2015. Available online: http://epcco.com/epc/CEOInsights/FastJustGotFasterBlog/December2013.aspx (accessed on 15 October 2017).
66. Casady, J. Power products commercial roadmap for SiC from 2012–2020. In Proceedings of the US DOE High MW Direct-Drive Motor Workshop, Gaithersburg, MD, USA, 4 September 2014.
67. Waide, P.; Brunner, C. *Energy-Efficiency Policy Opportunities for Electric Motor-Driven Systems*; IEA: Paris, France, 2011.
68. Research, G. Global Electric Motor Sales Market Size Report, 2021–2028. Grandviewresearch.com. 2018. Available online: https://www.grandviewresearch.com/industry-analysis/electric-motor-market?utm_source=wordpress&utm_medium=social&utm_campaign=Gaurav_July3_ict_ElectricDCMotor_RD2&utm_content=Content (accessed on 18 July 2019).
69. Goetzler, W.; Sutherland, T.; Reis, C. *Energy Savings Potential and Opportunities for High-Efficiency Electric Motors in Residential and Commercial Equipment*; OSTI: Oak Ridge, TN, USA, 2013.
70. McCoy, G.A.; Douglass, J.G. *Premium Efficiency Motor Selection and Application Guide—A Handbook for Industry*; US Department of Energy: Washington, DC, USA, 2014.
71. Kizilyalli Isik, C.; Carlson Eric, P.; Cunningham Daniel, W.; Manser Joseph, S.; Xu, Y.; Liu, A.Y. Wide Band-Gap Semiconductor Based Power Electronics for Energy Efficiency. ARPA.e, 13 March 2018. Available online: https://arpa-e.energy.gov/sites/default/files/documents/files/ARPA-E_Power_Electronics_Paper-April2018.pdf (accessed on 28 October 2014).
72. Lowe, M.; Golini, R.; Gereffi, G. US Adoption of High-Efficiency Motors and Drives: Lessons Learned. Durham, NC. 2010. Available online: http://www.cggc.duke.edu/pdfs/CGGC-Motor_and_Drives_Report_Feb_25_2010.pdf (accessed on 28 October 2014).
73. Kohei, S.; Swamy, M.; Kang, J.K.; Hisatsune, M.; Wu, Y.; Kebort, D.; Honea, J. Advantages of High Frequency PWM in AC Motor Drive Applications. In Proceedings of the 2012 IEEE Energy Conversion Congress and Exposition, ECCE 2012, Raleigh, NC, USA, 15–20 September 2012; pp. 2977–2984. [CrossRef]
74. Jahns, T. The Past, Present, and Future of Power Electronics Integration Technology in Motor Drives. *CPSS Trans. Power Electron. Appl.* **2017**, *2*, 197–216. [CrossRef]
75. Di, H.; Ogale, A.; Li, S.; Li, Y.; Sarlioglu, B. Efficiency Characterization and Thermal Study of GaN Based 1 kW Inverter. In Proceedings of the IEEE Applied Power Electronics Conference and Exposition—APEC, Fort Worth, TX, USA, 16–20 March 2014; pp. 2344–2350. [CrossRef]
76. Rice, J.; Mookken, J. Economics of High Efficiency SiC MOSFET Based 3-Ph Motor Drive. In Proceedings of the PCIM Europe 2014: International Exhibition and Conference for Power Electronics, Intelligent Motion, Renewable Energy and Energy Management, Nuremberg, Germany, 20–22 May 2014; pp. 1003–1010.
77. Vogel, K.; Rossa, A.J. Improving Efficiency in AC Drives: Comparison of Topologies and Device Technologies. In Proceedings of the PCIM Europe 2014: International Exhibition and Conference for Power Electronics, Intelligent Motion, Renewable Energy and Energy Management, Nuremberg, Germany, 20–22 May 2014; pp. 509–516.
78. Ozpineci, B. Oak Ridge National Laboratory Annual Progress Report for the Power Electronics and Electric Motors Program. 2015. Available online: http://info.ornl.gov/sites/publications/files/Pub59624.pdf (accessed on 26 July 2023).
79. Sten, K.; Kushnir, D. How Energy Efficient Is Electrified Transport. In *Systems Perspectives on Electromobility*; Sandén, B., Wallgren, P., Eds.; Chalmers University of Technology: Gothenburg, Sweden, 2013; p. 184. Available online: https://publications.lib.chalmers.se/records/fulltext/179113/local_179113.pdf (accessed on 26 July 2023).
80. Mitova, R.; Ghosh, R.; Mhaskar, U.; Klikic, D.; Wang, M.; Dentella, A. Investigations of 600-V GaN HEMT and GaN Diode for Power Converter Applications. *IEEE Trans. Power Electron.* **2014**, *29*, 2441–2452. [CrossRef]
81. Burger, B.; Kranzer, D.; Stalter, O. Cost Reduction of PV-Inverters with SiC-DMOSFETs. In Proceedings of the 2008 5th International Conference on Integrated Power Systems, Nuremberg, Germany, 11–13 March 2008.
82. Stubbe, T.; Kunze, M. GaN Power Semiconductors for PV Inverter Applications—Opportunities and Risks. In Proceedings of the CIPS 2014: 8th International Conference on Integrated Power Electronics Systems, Nuremberg, Germany, 25–27 February 2014.
83. Shiozaki, K.; Toshiyuki, K.; Lee, J.; Miyagi, K. *Verification of High Frequency SiC On-Board Vehicle Battery Charger for PHV*; SAE Technical Paper 2016-01-1210; SAE: Warrendale, PA, USA, 2016.
84. Su, G.-J.; Tang, L. An integrated onboard charger and accessory power converter using WBG devices. In Proceedings of the 2015 IEEE Energy Conversion Congress and Exposition (ECCE), Montreal, QC, Canada, 20–24 September 2015; pp. 6306–6313.
85. EV Everywhere: Grand Challenge Blueprint. 31 January 2013. Available online: https://www.energy.gov/sites/prod/files/2014/02/f8/eveverywhere_blueprint.pdf (accessed on 26 July 2023).
86. Ricardo, F.; Moura, P.; Delgado, J.; De Almeida, A.T. A Sustainability Assessment of Electric Vehicles as a Personal Mobility System. *Energy Convers. Manag.* **2012**, *61*, 19–30. [CrossRef]
87. Chinthavali, M.; Otaduy, P.; Ozpineci, B. Comparison of Si and SiC Inverters for IPM Traction Drive. In Proceedings of the 2010 IEEE Energy Conversion Congress and Exposition, Atlanta, GA, USA, 12–16 September 2010; pp. 3360–3365. [CrossRef]
88. Hamada, K.; Nagao, M.; Ajioka, M.; Kawai, F. SiC-emerging power device technology for next-generation electrically powered environmentally friendly vehicles. *IEEE Trans. Electron. Devices* **2015**, *62*, 278–285. [CrossRef]
89. Su, M.; Chen, C.; Sharma, S.; Kikuchi, J. Performance and cost considerations for SiC-based HEV traction inverter systems. In Proceedings of the 2015 IEEE 3rd Workshop on Wide Bandgap Power Devices and Applications (WiPDA), Blacksburg, VA, USA, 2–4 November 2015; pp. 347–350.
90. Williams, J.; Haley, B.; Kahrl, F.; Moore, J.; Jones, A.; Torn, M.; McJeon, H. *Pathways to Deep Decarbonization in the United States*; Energy and Environmental Economics, Inc.: San Francisco, CA, USA, 2014.

91. Sadik, O.; Acar, F.; Selamogullari, U.S. Comparison of Silicon Carbide MOSFET and IGBT Based Electric Vehicle Traction Inverters. In Proceedings of the 2015 International Conference on Electrical Engineering and Informatics (ICEEI), Denpasar, Indonesia, 10–11 August 2015. [CrossRef]
92. Pierre, D.; Whitney, J. Data Center Efficiency Assessment. 2014. Available online: http://www.nrdc.org/energy/data-center-efficiency-assessment.asp (accessed on 26 July 2023).
93. Brown, R.; Masaet, E.; Nordman, B.; Shehabi, B.T.A.; Stanley, J.; Koomey, J.; Sartor, P.; Chan, P.; Alliance to Save Energy; ICF Incorporated; et al. *Report to Congress on Server and Data Center Energy Efficiency: Public Law 109–431*; Lawrence Berkeley National Laboratory: Berkeley, CA, USA, 2007. Available online: https://www.osti.gov/servlets/purl/929723 (accessed on 26 July 2023).
94. Scheihing, P. DOE Data Center Energy Efficiency Program. April 2009. Available online: https://www1.eere.energy.gov/manufacturing/tech_assistance/pdfs/doe_data_centers_presentation.pdf (accessed on 26 July 2023).
95. Pearsall, N.M. Introduction to photovoltaic system performance. In *The Performance of Photovoltaic (PV) Systems*; Woodhead Publishing: Cambridge, UK, 2017; pp. 1–19.
96. Masanet, E.R.; Brown, R.E.; Shehabi, A.; Koomey, J.G.; Nordman, B. Estimating the Energy Use and Efficiency Potential of U.S. Data Centers. *Proc. IEEE* **2011**, *99*, 1440–1453. [CrossRef]
97. Simonetti, V. *Lo Standard a Protezione Dell'ambiente e Dei Consumatori: Un Caricabatterie Comune per Gli Stati Membri UE*; Luiss Guido Carli: Rome, Italy, 2022.
98. Eykyn, J. *The World Market for AC-DC & DC-DC Merchant Power Supplies—2013 Edition*; IHS: Wellingborough, UK, 2013; Volume 9790.
99. Huston, E.; Swisher, J.; Burns, C.; Seal, J.; Emerson, B. *Design Recommendations for High-Performance Data Centers*; Rocky Mountain Institute: Snowmass, CO, USA, 2003.
100. Morrow, L. Mitsubishi Electric Introduces New SUMMIT Series UPS. *Mission Critical*, 8 September 2015.
101. ORNL. *Power Electronics for Distributed Energy Systems and Transmission and Distribution Applications*; ORNL: Oak Ridge, TN, USA, 2006.
102. SMA Solar Technology. *Technical Information Efficiency and Derating WKG-Derating-US-TI-en-15 Version 1.5*; SMA Solar Technology: Niestetal, Germany, 2016.
103. EIA. Annual Energy Outlook 2013. Available online: http://www.eia.gov/forecasts/aeo/ (accessed on 26 July 2023).
104. McDonald, T. Impact of Commercialization of GaN based Power Devices on PV Solar Power 625 Generation. International Rectifier. 2011. Available online: http://www.arpa-626e.energy.gov/sites/default/files/documents/files/SolarADEPT_Workshop_NxtGenPwr_McDonald.pdf (accessed on 26 July 2023).
105. NREL. 2012 Renewable Energy Data Book. 2012. Available online: http://www.nrel.gov/docs/fy14osti/60197.pdf (accessed on 26 July 2023).
106. Zhang, H.; Tolbert, L.M.; Ozpineci, B. Impact of SiC Devices on Hybrid Electric and Plug-In Hybrid Electric Vehicles. *IEEE Trans. Ind. Appl.* **2011**, *47*, 912–921. [CrossRef]
107. Yu, L.; Dunne, G.; Matocha, K.; Cheung, K.; Suehle, J.; Sheng, K. Reliability Issues of SiC MOSFETs: A Technology for High-Temperature Environments. *IEEE Trans. Device Mater. Reliab.* **2010**, *10*, 418–426. [CrossRef]
108. Ellis, M.; Jollands, N. *Gadgets and Gigawatts: Policies for Energy Efficient Electronics*; International Energy Agency: Paris, France, 2009. Available online: https://www.iea.org/reports/gadgets-and-gigawatts-2 (accessed on 26 July 2023).

Disclaimer/Publisher's Note: The statements, opinions and data contained in all publications are solely those of the individual author(s) and contributor(s) and not of MDPI and/or the editor(s). MDPI and/or the editor(s) disclaim responsibility for any injury to people or property resulting from any ideas, methods, instructions or products referred to in the content.